Bollettino
Unione Matematica Italiana

Luca F. Pavarino

Domain decomposition methods and scientific computing applications

Bollettino dell'Unione Matematica Italiana, Serie 8, Vol. **8-B** (2005), n.1, p. 21–54.

Unione Matematica Italiana

<http://www.bdim.eu/item?id=BUMI_2005_8_8B_1_21_0>

Bollettino dell'Unione Matematica Italiana, Unione Matematica Italiana, 2005.

Bollettino U. M. I.
(8) 8-B (2005), 21-54

Domain Decomposition Methods and Scientific Computing Applications.

LUCA F. PAVARINO (*)

Sunto. – *Questo lavoro illustra le idee principali relative ai metodi di decomposizione dei domini e alla loro analisi di convergenza. Questi algoritmi sono dei metodi paralleli e scalabili per la risoluzione numerica efficiente di equazioni alle derivate parziali. Sono inoltre illustrati due esempi di applicazioni di metodi di decomposizione dei domini a simulazioni numeriche di grande scala in meccanica ed elettrocardiologia computazionale.*

Summary. – *This paper reviews the basic mathematical ideas and convergence analysis of domain decomposition methods. These are parallel and scalable iterative methods for the efficient numerical solution of partial differential equations. Two examples are then presented showing the application of domain decomposition methods to large-scale numerical simulations in computational mechanics and electrocardiology.*

1. – Introduction.

Domain decomposition methods are among the most popular and efficient methods for the numerical solution of large-scale problems based on partial differential equations. The main idea of these methods is to divide the original problem or its approximation into smaller subproblems, devising an iterative procedure that converges rapidly to the original solution. This idea can be applied directly to the continuous problem, to the discrete problem or to the resulting algebraic system. In the first two cases, domain decomposition methods are know as iteration-by-subdomain methods (see Quarteroni and Valli [36]), while in the latter they take the form of preconditioners accelerated by Krylov space methods (see Smith, Bjørstad and Gropp [38]). The recursive application of these techniques leads to multilevel domain decomposition

(*) Conferenza tenuta a Milano il 13 settebre 2004 in occasione del XVII Congresso U.M.I.

This work was supported in part by the National Science Foundation under Grant NSF-CCR-9732208 and in part by MIUR (PRIN 2001).

methods, including the older family of multigrid methods. The main motivations for domain decomposition methods have been the need to compute with parallel and distributed architectures, to subdivide domains with complicated geometries into simpler ones, and to consider different mathematical models and/or numerical methods on different parts of the domain. While the original motivations of the earlier works in this field were mainly theoretical (see Schwarz [37], Sobolev [39], Babuška [6], Lions [26]), much of the current interest and activity in domain decomposition methods has been driven by parallel computing for large-scale applications, particularly in the structural mechanics and fluid dynamics communities. Integrated in modular software libraries based on finite elements or finite differences, domain decomposition preconditioners have allowed iterative solvers to become competitive and in some cases dominant in large-scale simulations; see e.g. Keyes [23], Tufo and Fischer [41], Bhardway et al. [10], Akcelik et al. [4], and the references therein. The main goal of this paper is to present a brief review of the main domain decomposition techniques and to show some advanced applications where mathematical theory and parallel scientific computing merge into efficient large-scale solvers.

For a more complete treatment of domain decomposition methods, we refer to the books by Smith, Bjørstad and Gropp [38], Quarteroni and Valli [36], Toselli and Widlund [40], to the review papers by Chan and Mathew [13], Le Tallec [25], Farhat and Roux [18] and to the proceedings of the international conferences and workshops in the field, the last ones being [24, 21, 32]. There is also an official website at http://www.ddm.org. For a general introduction to numerical methods for partial differential equations, we refer to Quarteroni and Valli [35].

This paper starts with a brief review of the basic mathematical ideas of domain decomposition methods in Section 2. The abstract mathematical framework employed for the convergence analysis of these methods is briefly presented in Section 3. The paper then continues with two scientific computing applications. The first, presented in Section 4, extends the class of domain decomposition methods known as Balancing Neumann-Neumann methods to the linear elasticity and Stokes systems. The second application, presented in Section 5, concerns block Jacobi methods for reation-diffusion systems arising in computational electrocardiology.

2. – Basic ideas.

The basic domain decomposition ideas are best described in the simplest case involving only two subdomains, a second-order, self-adjoint, linear, elliptic operator (for simplicity the Laplacian) and homogeneous Dirichlet bounda-

ry conditions:

$$(1) \qquad \begin{cases} -\Delta u = f & \text{in } \Omega, \\ u = 0 & \text{on } \partial\Omega, \end{cases}$$

where e.g. $f \in L^2(\Omega)$ and $\partial\Omega$ is Lipschitz continuous. Using a standard Galerkin procedure based on a variational formulation of (1) and a discrete space V spanned by finite or spectral element functions, this continuous problem is approximated by a linear system

$$Au = f,$$

where we used the same notation for functions and the vectors of coefficients of their discrete approximations. $A_{ij} = \int_\Omega \nabla\phi_i \cdot \nabla\phi_j \, dx$ is the stiffness matrix, $f_j = \int_\Omega f\phi_j \, dx$ the load vector and $\{\phi_i\}_{i=1}^{\dim(V)}$ is a basis for the discrete space V. We will briefly illustrate the two main families of domain decomposition methods, based on nonoverlapping or overlapping decompositions of Ω; for more details see Toselli and Widlund [40, Ch. 1].

2.1. *Nonoverlapping methods.*

Let Ω be decomposed into two nonoverlapping subdomains $\overline{\Omega_1 \cup \Omega_2} = \overline{\Omega}$, $\Omega_1 \cap \Omega_2 = \emptyset$, and let $\Gamma = \partial\Omega_1 \cap \partial\Omega_2$ be their common interface. The original elliptic problem is then equivalent to the coupled problems (see Quarteroni and Valli [36])

$$\begin{cases} -\Delta u_i = f & \text{in } \Omega_i, \qquad i = 1, 2 \\ u_i = 0 & \text{su } \partial\Omega_i \setminus \Gamma \\ u_1 = u_2 & \text{on } \Gamma, \\ \dfrac{\partial u_1}{\partial n_1} = -\dfrac{\partial u_2}{\partial n_2} & \text{on } \Gamma \end{cases}$$

where n_i is the outward normal on $\partial\Omega_i$. The last two equations on Γ are known as transmission or interface conditions. We can obtain an analogous decomposition in the discrete case by partitioning the degrees of freedom into those internal to Ω_1, internal to Ω_2, and interior to Γ

$$u = \begin{bmatrix} u_I^1 \\ u_I^2 \\ u_\Gamma \end{bmatrix}, \quad f = \begin{bmatrix} f_I^1 \\ f_I^2 \\ f_\Gamma \end{bmatrix}, \quad A = \begin{bmatrix} A_{II}^1 & 0 & A_{I\Gamma}^1 \\ 0 & A_{II}^2 & A_{I\Gamma}^2 \\ A_{\Gamma I}^1 & A_{\Gamma I}^2 & A_{\Gamma\Gamma} \end{bmatrix}.$$

A and f are obtained by subassembling their local contributions

$$A_{\Gamma\Gamma} = A^1_{\Gamma\Gamma} + A^2_{\Gamma\Gamma}, \qquad f_\Gamma = f^1_\Gamma + f^2_\Gamma,$$

where

$$f^i = \begin{pmatrix} f^i_I \\ f^i_\Gamma \end{pmatrix}, \quad A^i = \begin{pmatrix} A^i_{II} & A^i_{I\Gamma} \\ A^i_{\Gamma I} & A^i_{\Gamma\Gamma} \end{pmatrix}, \quad i = 1, 2$$

are local load vectors and stiffness matrices for local problems on each Ω_i with Dirichlet data on $\Omega_i \setminus \Gamma$ and Neumann data on Γ. Using Green's formula to represent the functional $\int_\Gamma \frac{\partial u_i}{\partial n_i} \phi_j \, ds$ associated with the normal derivative on Γ, we can see that its discrete approximation is

$$\lambda^i = A^i_{\Gamma I} u^i_I + A^i_{\Gamma\Gamma} u^i_\Gamma - f^i_\Gamma.$$

With these notations, the discrete problem can be decomposed as

$$\begin{cases} A^i_{II} u^i_I + A^i_{I\Gamma} u^i_\Gamma = f^i_I \; i = 1, 2 & (i) \\ u^1_\Gamma = u^2_\Gamma = u_\Gamma & (D) \\ A^1_{\Gamma I} u^1_I + A^1_{\Gamma\Gamma} u^1_\Gamma - f^1_\Gamma = -(A^2_{\Gamma I} u^2_I + A^2_{\Gamma\Gamma} u^2_\Gamma - f^2_\Gamma) = \lambda_\Gamma & (N) \end{cases}$$

(i) + (D) are local problems with zero Dirichlet data on $\partial\Omega_i \setminus \Gamma$ e u_Γ su Γ, while (i) + (N) are local problems with zero Dirichlet data on $\partial\Omega_i \setminus \Gamma$ and Neumann data λ_Γ on Γ. It is possible to reduce the discrete problem to a problem for u_Γ only, known as the Schur complement system, or to a problem for the discrete flux λ_Γ only, known as the flux or FETI system. The first one is obtained by eliminating the interior unknowns u^i_I in the Dirichlet problems (i) + (D) and substituting the resulting expression into (N). The reduced system is then

$$Su_\Gamma = g_\Gamma, \qquad \text{where}$$

$$S = A_{\Gamma\Gamma} - A^1_{\Gamma I} A^{1^{-1}}_{II} A^1_{I\Gamma} - A^2_{\Gamma I} A^{2^{-1}}_{II} A^2_{I\Gamma} = S^1 + S^2$$

is the Schur complement of A and

$$g_\Gamma = g^1_\Gamma + g^2_\Gamma, \quad g^i_\Gamma = f^i_\Gamma - A^i_{\Gamma I} A^{i^{-1}}_{II} f^i_I, \quad i = 1, 2.$$

Once u_Γ is found, the internal unknowns are determined by solving the decoupled Dirichlet problems

$$u^i_I = A^{i^{-1}}_{II} (f^i_I - A^i_{I\Gamma} u_\Gamma).$$

Alternatively, a system for the discrete flux is obtained by eliminating the in-

terior unknowns u_I^i in the local Neumann problems (i) + (N)

$$\begin{pmatrix} A_{II}^i & A_{I\Gamma}^i \\ A_{\Gamma I}^i & A_{\Gamma\Gamma}^i \end{pmatrix} \begin{pmatrix} u_I^i \\ u_\Gamma^i \end{pmatrix} = \begin{pmatrix} f_I^i \\ f_\Gamma^i + \lambda_\Gamma^i \end{pmatrix}, \quad i = 1, 2.$$

We find $u_\Gamma^i = S^{i^{-1}}(g_\Gamma^i + \lambda_\Gamma^i)$ and substituting into (D) we obtain the flux system

$$(S^{1^{-1}} + S^{2^{-1}})\,\lambda_\Gamma = d_\Gamma,$$

with $d_\Gamma = -S^{1^{-1}} g_\Gamma^1 + S^{2^{-1}} g_\Gamma^2$. While either the Schur complement or discrete flux systems could be solved directly by explicitly assembling the relative matrices, a more efficient strategy consists in solving these systems iteratively, starting with an initial guess and using a Krylov space method where only matrix-vector products are required. We illustrate this strategy with the Neumann-Neumann method for the Schur complement system. Many other choices are possible, among which are the Dirichlet-Neumann and FETI Dirichlet-Dirichlet methods; see [40].

2.1.1. Neumann-Neumann method. – At the continuous level, the Neumann-Neumann iteration starts from an initial guess u_Γ^0, solves on each Ω_i a Dirichlet problem with data u_Γ^0 on Γ and then on each Ω_i a Neumann problem with data on Γ equal to the sum of the normal derivatives of the previous Dirichlet solutions. The new iterate u_Γ^1 is then built from the values on Γ of the Neumann solutions. More precisely

$$(D_i) \left\{ \begin{array}{lll} -\Delta u_i^{n+1/2} = f & \text{in } \Omega_i, \\ u_i^{n+1/2} = 0 & \text{on } \partial\Omega_i \setminus \Gamma \\ u_i^{n+1/2} = u_\Gamma^n & \text{on } \Gamma \end{array} \right\} \quad i = 1, 2$$

$$(N_i) \left\{ \begin{array}{lll} -\Delta u_i^{n+1} = 0 & & \text{in } \Omega_i, \\ u_i^{n+1} = 0 & & \text{on } \partial\Omega_i \setminus \Gamma \\ \dfrac{\partial u_i}{\partial n_i^{n+1}} = \dfrac{\partial u_1}{\partial n_1^{n+1/2}} + \dfrac{\partial u_2}{\partial n_2^{n+1/2}} & & \text{on } \Gamma \end{array} \right\} \quad i = 1, 2,$$

We then update $u_\Gamma^{n+1} = u_\Gamma^n - \theta(u_1^{n+1} + u_2^{n+1})$ on Γ, where $\theta \in (0, \theta_{\mathrm{MAX}})$ is a suitable constant. At the discrete level, this method can be written

$$(D_i) \quad A_{II}^i u_I^{i,\,n+1/2} + A_{I\Gamma}^i u_\Gamma^n = f_I^i \quad i = 1, 2$$

$$(N_i) \quad \begin{pmatrix} A_{II}^i & A_{I\Gamma}^i \\ A_{\Gamma I}^i & A_{\Gamma\Gamma}^i \end{pmatrix} \begin{pmatrix} u_I^{i,\,n+1} \\ u_\Gamma^{i,\,n+1} \end{pmatrix} = \begin{pmatrix} 0 \\ r_\Gamma \end{pmatrix} \quad i = 1, 2,$$

$$u_\Gamma^{n+1} = u_\Gamma^n - \theta(u_\Gamma^{1,\,n+1} + u_\Gamma^{2,\,n+1}),$$

where

$$r_\Gamma = (A_{\Gamma I}^1 u_I^{1,\,n+1/2} + A_{\Gamma\Gamma}^1 u_\Gamma^n - f_\Gamma^1) + (A_{\Gamma I}^2 u_I^{2,\,n+1/2} + A_{\Gamma\Gamma}^2 u_\Gamma^n - f_\Gamma^2).$$

Eliminating the interior unknowns $u_I^{i,\,n+1/2}$ in the Dirichlet problems (D_i) we obtain $r_\Gamma = -(g_\Gamma - Su_\Gamma^n)$, while eliminating $u_I^{i,\,n+1}$ in the Neumann problems (N_i) we obtain $u_\Gamma^{i,\,n+1} = S^{i^{-1}} r_\Gamma$. Therefore

$$u_\Gamma^{n+1} - u_\Gamma^n = \theta(S^{1^{-1}} + S^{2^{-1}})(g_\Gamma - Su_\Gamma^n),$$

which is a Richardson iteration for the Schur complement $Su_\Gamma = g_\Gamma$ with preconditioner $S^{1^{-1}} + S^{2^{-1}}$. In the computational practice, it is best to substitute the slower Richardson iteration with a faster Krylov space method such as the preconditioned conjugate gradient method. It is also possible to scale the right-hand sides of the Neumann problems and the update equation with positive weights $\delta_1^\dagger$, $\delta_2^\dagger$ that sum to 1, obtaining the preconditioner

$$D^1 S^{1^{-1}} D^1 + D^2 S^{2^{-1}} D^2,$$

where D^i are diagonal scaling matrices with diagonal elements equal to $\delta_i^\dagger$.

2.2. *Overlapping methods*

The other main family of domain decomposition methods is based on decomposing Ω into overlapping subdomains Ω_1', Ω_2'. The classical alternating (or multiplicative) Schwarz algorithm al the continuous level consists in alternatively solving Dirichlet problems on each overlapping subdomain using as boundary data the trace of the previous Dirichlet solution in the other subdomain

$$(1)\quad \begin{cases} -\Delta u^{n+1/2} = f & \text{in } \Omega_1', \\ u^{n+1/2} = u^n & \text{on } \partial\Omega_1' \text{ and outside } \Omega_1' \end{cases}$$

$$(2)\quad \begin{cases} -\Delta u^{n+1} = f & \text{in } \Omega_2', \\ u^{n+1} = u^{n+1/2} & \text{on } \partial\Omega_2' \text{and outside } \Omega_2'. \end{cases}$$

Using the variation formulation of the algorithm based on the associated bilinear form $a(u, v) = \int_\Omega \nabla u \cdot \nabla v dx$, one finds the error equation

$$u^{n+1} - u = (I - P_2)(I - P_1)(u^n - u),$$

where P_i: $H_0^1(\Omega) \to H_0^1(\Omega_i')$ are orthogonal projections defined by

$$a(P_i u, v) = a(u, v) \qquad \forall v \in H_0^1(\Omega_i').$$

Hence the error propagation operator is

$$(I - P_2)(I - P_1) = I - (P_1 + P_2 - P_2 P_1)$$

and the multiplicative Schwarz algorithm consists in solving iteratively

$$P_{ms}\, u = (P_1 + P_2 - P_2 P_1)\, u = g\ ,$$

where $g \in V$ is chosen so that u is the solution of the original discrete problem. Since the two local solutions in the algorithm are sequential, we can define the more parallel additive Schwarz algorithm

$$P_{as}\, u = (P_1 + P_2)\, u = g\ ,$$

with g again properly chosen. A Richardson iteration for this additive Schwarz system in general does not converge, so a Krylov space acceleration is here essential.

2.3. *Many subdomains and coarse solvers.*

In practice, many more than two subdomains are often required. All the domain decomposition methods we have mentioned can be extended to decompositions with N (overlapping or nonoverlapping) subdomains, $\Omega = \bigcup_{i=1}^{N} \Omega_i$. For example, the Neumann-Neumann preconditioned operator becomes

$$S_{NN}^{-1} S = \sum_{i=1}^{N} D_i^T S^{i\dagger} D_i S\ ,$$

(the pseudoinverses $S^{i\dagger}$ are required for Neumann solves on interior subdomains that do not have any Dirichlet boundary), the multiplicative Schwarz operator

$$P_{ms} = I - (I - P_N) \ldots (I - P_1)\,,$$

and the additive Schwarz operator

$$P_{as} = \sum_{i=1}^{N} P_i .$$

It is possible to prove that for elliptic problems, these one-level methods are not scalable, i.e. the number of iterations required to converge to a desired accuracy is proportional to the number of subdomains N. Therefore, two-level or multilevel extensions must be considered. In the computational practice, two-level methods have so far offered the best compromise between simplicity and performance, but things could have to be reconsidered as the number of processors in current parallel architectures keeps increasing. In two-level methods, a coarse solver is usually associated with a global problem with a few unknowns per subdomain. Its design can be quite complex in nonoverlapping

methods such as the Neumann-Neumann method, where one of the most popular two-level versions, known as the Balancing Neumann-Neumann method (see Mandel and Brezina [28]), employs a coarse solver S_0 in multiplicative form and local solvers in additive form

$$S_{NN}^{-1} = S_0 + (I - S_0 S)\left(\sum_{i=1}^{N} D_i^T S^{i\dagger} D_i\right)(I - S S_0).$$

In overlapping methods, a more standard coarse solver P_0 can be employed, yielding the two-level multiplicative Schwarz operator

$$P_{ms} = I - (I - P_N)\ldots(I - P_1)(I - P_0)$$

and the two-level additive Schwarz operator

$$P_{as} = \sum_{i=0}^{N} P_i.$$

3. – Classical Schwarz theory.

The convergence properties of domain decomposition methods can be studied using an abstract framework known as abstract Schwarz theory. We recall here the main features of this theory and we refer, e.g, to Toselli and Widlund [40] or Smith, Bjørstad and Gropp [38] for a more complete treatment.

Let V be a finite dimensional Hilbert space, $a(\cdot, \cdot): V \times V \to R$ a symmetric, positive definite bilinear form and f a linear functional over V. We want to solve the discrete problem: find $u \in V$ such that

$$a(u, v) = f(v) \qquad \forall v \in V. \tag{2}$$

Given a basis in V and using the same notation for functions (or functionals) and the associated vectors of degrees of freedom, this problem is equivalent to the linear system

$$Au = f,$$

where A is the symmetric, positive definite stiffness matrix associated with $a(\cdot, \cdot)$. Given a family of spaces $\{V_i, i = 0, \ldots, N\}$ and interpolation (or extension) operators $R_i^T: V_i \to V$, we assume that V can be decomposed into $N + 1$ subspaces:

$$V = R_0^T V_0 + R_1^T V_1 + \ldots + R_N^T V_N.$$

Even if the spaces V_i need not be subspaces of V, the usual terminology in domain decomposition theory refers to them as subspaces; usually V_0 is a global

subspace related to a coarse problems associated with a coarse mesh, while V_i, $i = 1, \dots, N$ are local subspaces associated with local meshes. For each subspace, we assume that there is a symmetric, positive definite bilinear form

$$a_i(\cdot, \cdot) : V_i \times V_i \to R$$

with associated local stiffness matrix $A_i : V_i \to V_i$. If we use the original bilinear form (i.e. we use local exact solvers)

$$a_i(u_i, v_i) = a(R_i^T u_i, R_i^T v_i), \qquad u_i, v_i \in V_i,$$

then $A_i = R_i A R_i^T$. We define projection-like operators

$$P_i = R_i^T \tilde{P}_i : V \to R_i^T V_i, \qquad i = 0, \dots, N$$

where $\tilde{P}_i : V \to V_i$ is defined by

$$a_i(\tilde{P}_i u, v_i) = a(u, R_i^T v_i), \qquad v_i \in V_i.$$

It is easy to prove (see [40, Lemma 2.2.1]) that

$$P_i = R_i^T A_i^{-1} R_i A, \qquad i = 0, \dots, N,$$

and that the operators P_i are self-adjoint in the inner product defined by $a(\cdot, \cdot)$ and positive semi-definite. In case of exact local solvers, they are actually projections.

With these operators, defined by the choice of subspaces and local bilinear forms, we can build domain decomposition methods by considering Schwarz operators defined in terms of polynomials in P_i without zero order terms. We have the additive Schwarz operator

$$P_A = P_0 + P_1 + \dots + P_N,$$

the multiplicative Schwarz operator

$$P_M = I - (I - P_N)(I - P_{N-1}) \dots (I - P_0),$$

and many hybrid operators combining additive and multiplicative terms, such as the balancing Neumann-Neumann operator

$$P_{NN} = I - (I - P_0) \left(I - \sum_{i=1}^{N} P_i \right) (I - P_0).$$

In case of exact coarse solver on V_0, this last operator can be written as

$$P_{NN} = P_0 + (I - P_0) \sum_{i=1}^{N} P_i (I - P_0).$$

All these Schwarz operators define preconditioned operators for the original operator A, i.e. they can be written as the product of a suitable preconditioner

and A. For example, in the easier additive case,

$$P_A = B_A^{-1} A, \quad \text{where} \quad B_A^{-1} = \sum_{i=0}^{N} R_i^T A_i^{-1} R_i$$

and analogous formulae hold for multiplicative and hybrid operators. The convergence theory of Schwarz methods is based on the following three hypotheses.

ASSUMPTION 1 (Stable decomposition). – *There exists a constant* C_0 *such that every* $v \in V$ *admits a decomposition* $v = \sum_{i=0}^{N} R_i^T v_i$, $v_i \in V_i$, *that satisfies*

$$\sum_{i=0}^{N} a_i(v_i, v_i) \leq C_0^2 a(v, v).$$

ASSUMPTION 2 (Strengthened Cauchy-Schwarz inequality). – *There exist constants* $0 \leq \varepsilon_{ij} \leq 1$, $i, j = 1, \ldots, N$ *such that*

$$a(R_i^T v_i, R_j^T v_j) \leq \varepsilon_{ij} a(R_i^T v_i, R_i^T v_i)^{1/2} a(R_j^T v_j, R_j^T v_j)^{1/2} \quad \forall v_i \in V_i, \quad \forall v_j \in V_j.$$

We will denote by $\varrho(\mathcal{E})$ *the spectral radius of* $\mathcal{E} = \{\varepsilon_{ij}\}$.

ASSUMPTION 3 (Local stability). – *There exists a constant* $\omega > 0$ *such that for* $i = 0, 1, \ldots, N$,

$$a(R_i^T v_i, R_i^T v_i) \leq \omega a_i(v_i, v_i) \qquad \forall v_i \in \text{Range}\,(\tilde{P}_i) \subset V_i.$$

The main convergence result for the additive operator P_A provides a bound for its condition number $\kappa(P_A) = \lambda_{\max}(P_A)/\lambda_{\min}(P_A)$

THEOREM 1. – *If Assumptions* 1,2,3 *are satisfied, then*

$$\kappa(P_A) \leq C_0^2 \omega(\varrho(\mathcal{E}) + 1).$$

The main convergence result for the multiplicative operator provides a bound for the a-norm of its associated error propagation operator $I - P_M$.

THEOREM 2. – *If Assumptions* 1,2,3 *are satisfied and* $\omega \in (0, 2)$, *then*

$$\|I - P_M\|_a^2 \leq 1 - \frac{2 - \omega}{C_0^2 (2\,\tilde{\omega}^2 \varrho(\mathcal{E})^2 + 1)} < 1,$$

where $\tilde{\omega} = \max\{1, \omega\}$.

In order to obtain a convergence result for the hybrid operator P_{NN}, it is convenient to modify Assumption 1 as follows.

ASSUMPTION 1bis (Stable decomposition). – *There exists a constant* C_0 *such that every* $v \in \mathrm{Range}\,(I - P_0)$ *admits a decomposition* $v = \sum_{i=1}^{N} R_i^T v_i$, $v_i \in V_i$, *that satisfies*

$$\sum_{i=1}^{N} a_i(v_i, v_i) \leq C_0^2\, a(v, v)\,.$$

Then we have:

THEOREM 3. – *If Assumptions* 1bis,2,3 *are satisfied, then*

$$\max\{1, C_0^2\}^{-1}\, a(v, v) \leq a(P_{NN} v, v) \leq \max\{1, \omega\varrho(\mathcal{E})\}\, a(v, v)\,.$$

By estimating the constants C_0, $\varrho(\mathcal{E})$, ω for specific choices of subspaces and local bilinear forms, associated with specific domain decomposition algorithms, it is then possible to get concrete convergence rate estimates; see [40, 38, 16, 17].

4. – Application 1: Balancing Neumann-Neumann methods for elasticity and Stokes problems.

The balancing Neumann-Neumann algorithm can be extended to the linear elasticity and Stokes systems; see Pavarino and Widlund [34] and Goldfeld, Pavarino and Widlund [20] for a complete treatment with full proofs. Other nonoverlapping methods for elliptic systems can be found in [33], which extends previous works [30, 31] on scalar problems. Let $\Omega \subset R^3$ be a polyhedral domain, Γ_0 a nonempty subset of its boundary and $\widetilde{\boldsymbol{V}} = \{\boldsymbol{v} \in H^1(\Omega)^3 \colon \boldsymbol{v}\,|_{\Gamma_0} = 0\}$. The linear elasticity problem, with constant Lamé parameters, consists in finding the displacement $\boldsymbol{u} \in \widetilde{\boldsymbol{V}}$ of the domain Ω, fixed along Γ_0, subject to a surface force of density $\boldsymbol{g}$, along $\Gamma_1 = \partial\Omega \backslash \Gamma_0$, and a body force $\boldsymbol{f}$:

$$2\mu \int_{\Omega} \varepsilon(\boldsymbol{u}) \colon \varepsilon(\boldsymbol{v})\, dx + \lambda \int_{\Omega} \mathrm{div}\,\boldsymbol{u}\, \mathrm{div}\,\boldsymbol{v}\, dx = \langle \boldsymbol{F}, \boldsymbol{v} \rangle \quad \forall \boldsymbol{v} \in \widetilde{\boldsymbol{V}}. \tag{3}$$

Here λ and μ are the Lamé constants, $\varepsilon_{ij}(\boldsymbol{u}) = \frac{1}{2}\left(\frac{\partial u_i}{\partial x_j} + \frac{\partial u_j}{\partial x_i}\right)$ the linearized strain tensor, and the bilinear forms are defined as

$$\varepsilon(\boldsymbol{u}) \colon \varepsilon(\boldsymbol{v}) = \sum_{i=1}^{3} \sum_{j=1}^{3} \varepsilon_{ij}(\boldsymbol{u})\, \varepsilon_{ij}(\boldsymbol{v}), \quad \langle \boldsymbol{F}, \boldsymbol{v} \rangle = \int_{\Omega} \sum_{i=1}^{3} f_i v_i\, dx + \int_{\Gamma_1} \sum_{i=1}^{3} g_i v_i\, ds\,.$$

In Sections 4.5 and 4.6, we will consider the case of variable Lamé parameters and show that our algorithms are quite robust. The Lamé parameters can alternatively be expressed in terms of the Poisson ratio ν and Young's modu-

lus E:

$$\lambda = \frac{E\nu}{(1+\nu)(1-2\nu)}, \qquad \mu = \frac{E}{2(1+\nu)}.$$

When the material is almost incompressible, the Poisson ratio ν approaches the value $1/2$, i.e., λ/μ approaches infinity. In such cases, finite or spectral element discretizations of this pure displacement formulation suffer increasingly from locking phenomena and the resulting stiffness matrices become increasingly ill-conditioned. A possible remedy is based on introducing the new variable $p = -\lambda \operatorname{div} \boldsymbol{u} \in L^2(\Omega) = \widetilde{U}$ that we will call pressure and replacing the pure displacement problem with a mixed formulation: find $(\boldsymbol{u}, p) \in \widetilde{\boldsymbol{V}} \times \widetilde{U}$ such that

$$(4) \qquad \begin{cases} 2\mu \int_\Omega \varepsilon(\boldsymbol{u}) : \varepsilon(\boldsymbol{v})\, dx - \int_\Omega \operatorname{div} \boldsymbol{v} p\, dx = \langle \boldsymbol{F}, \boldsymbol{v} \rangle \quad \forall \boldsymbol{v} \in \widetilde{\boldsymbol{V}} \\ \qquad - \int_\Omega \operatorname{div} \boldsymbol{u} q\, dx - 1/\lambda \int_\Omega pq\, dx = \quad 0 \qquad \forall q \in \widetilde{U}; \end{cases}$$

see Brezzi and Fortin [11]. In the case of homogeneous Dirichlet boundary conditions for $\boldsymbol{u}$, we choose $\widetilde{U} = L_0^2(\Omega) = \{q \in L^2(\Omega) : \int_\Omega q dx = 0\}$, since it can be shown that the pressure will have zero mean value. We can also consider more general saddle point problems with a penalty term: find $(\boldsymbol{u}, p) \in \widetilde{\boldsymbol{V}} \times \widetilde{U}$ such that

$$(5) \qquad \begin{cases} a(\boldsymbol{u}, \boldsymbol{v}) + \quad b(\boldsymbol{v}, p) \quad = \langle \boldsymbol{F}, \boldsymbol{v} \rangle \quad \forall \boldsymbol{v} \in \widetilde{\boldsymbol{V}} \\ b(\boldsymbol{u}, q) - 1/\lambda\, c(p, q) = \quad 0 \qquad \forall q \in \widetilde{U}; \end{cases}$$

see Brezzi and Fortin [11]. In our specific case, we have

$$a(\boldsymbol{u}, \boldsymbol{v}) = 2\mu \int_\Omega \varepsilon(\boldsymbol{u}) : \varepsilon(\boldsymbol{v})\, dx, \quad b(\boldsymbol{v}, q) = -\int_\Omega \operatorname{div} \boldsymbol{v} q\, dx, \quad c(p, q) = \int_\Omega pq\, dx.$$

By letting $\lambda/\mu \to \infty$, we obtain the limiting problem for incompressible linear elasticity or the classical Stokes system for an incompressible fluid. A penalty term as in the compressible case can also originate from stabilization techniques or penalty formulations for Stokes problems.

4.1. *Discrete problem.*

We will consider conforming discretizations of Stokes and mixed elasticity equations using finite as well as spectral finite elements, all with discontinuous pressures. We assume that the domain Ω can be decomposed into N nonoverlapping subdomains Ω_i of characteristic size H forming a hexahedral

(quadrilateral) finite element mesh τ_H, which is assumed to be shape regular but not necessarily quasi uniform. This coarse triangulation is further refined into a fine quadrilateral finite element triangulation τ_h of characteristic size h. Among the many choices of mixed finite elements available for Stokes and mixed elasticity equations, we consider the following.

a) $Q_2(h) - Q_0(h)$ *mixed finite elements.* The displacement space $\tilde{\boldsymbol{V}}$ is discretized by continuous, piecewise bi-quadratic displacements:

$$\boldsymbol{V}^h = \{\boldsymbol{v} \in \tilde{\boldsymbol{V}} \colon v_k \,|_T \in Q_2(T) \ \ \forall T \in \tau_h, \ \ k = 1, 2, \ldots, d\},$$

while the pressure space is discretized by discontinuous piecewise constant functions

$$U^h = \{q \in \tilde{U} \colon q\,|_T \in Q_0(T) \ \ \forall T \in \tau_h\}.$$

These elements satisfy the uniform inf-sup condition

$$\sup_{\boldsymbol{v} \in \boldsymbol{V}^h} \frac{(\operatorname{div} \boldsymbol{v}, q)}{\|\boldsymbol{v}\|_{H^1}} \geqslant \beta_h \|q\|_{L^2} \quad \forall q \in U^h, \tag{6}$$

with $\beta_h \geqslant c > 0$ independent of h, but they lead to nonoptimal error estimates; see Brezzi and Fortin [11, Ch. VI.4, p. 221].

b) $Q_2(h) - P_1(h)$ *mixed finite elements.* The displacement space is as before, while the pressure space consists of piecewise linear discontinuous pressures:

$$U^h = \{q \in \tilde{U} \colon q\,|_T \in P_1(T) \ \ \forall T \in \tau_h\}.$$

These elements satisfy a uniform inf-sup condition (6) as well; there are also optimal $O(h^2)$ error estimates for both displacements and pressures; see Brezzi and Fortin [11, chap. VI, p. 216].

c) $Q_n - Q_{n-2}$ *mixed spectral elements.* We assume that the domain Ω can be decomposed into N nonoverlapping finite elements Ω_i, each of which is an affine image of the reference element $Q_n(\Omega_{\text{ref}}) = (-1, 1)^d$. $\tilde{\boldsymbol{V}}$ is discretized, component by component, by continuous, piecewise tensor product polynomials of degree n:

$$\boldsymbol{V}^n = \{\boldsymbol{v} \in \tilde{\boldsymbol{V}} \colon v_k \,|_{\Omega_i} \circ \phi_i \in Q_n(\Omega_{\text{ref}}), \ \ i = 1, 2, \ldots, N, \ \ k = 1, 2, \ldots, d\}.$$

The pressure space is discretized by piecewise tensor product polynomials of degree $n - 2$, which are discontinuous across the boundaries of the elements Ω_i:

$$U^n = \{q \in \tilde{U} \colon q\,|_{\Omega_i} \circ \phi_i \in Q_{n-2}(\Omega_{\text{ref}}), \ \ i = 1, 2, \ldots, N\}.$$

We use Gauss-Lobatto-Legendre (GLL(n)) quadrature in the implementation,

which also allows for the construction of a very convenient nodal tensor-product basis for $\boldsymbol{V}^n$. The $Q_n - Q_{n-2}$ method satisfies an inf-sup condition which is nonuniform in n but still satisfactory for practical values of $n \leq 16$. For an introduction to spectral methods and spectral elements, we refer to Canuto et al. [12] and Bernardi and Maday [9].

Let $\boldsymbol{V}$ and U be the discrete displacement and pressure spaces. In the finite element case, we write $\boldsymbol{V} \times U = \boldsymbol{V}^h \times U^h$, while in the spectral element case we have $\boldsymbol{V} \times U = \boldsymbol{V}^n \times U^n$. The discrete system obtained from (5) using finite or spectral elements is: find $\boldsymbol{u} \in \boldsymbol{V}$ and $p \in U$ such that

$$\text{(7)} \qquad \begin{cases} a(\boldsymbol{u}, \boldsymbol{v}) + \quad b(\boldsymbol{v}, p) \quad = \boldsymbol{F}(\boldsymbol{v}) \; \forall \boldsymbol{v} \in \boldsymbol{V} \\ b(\boldsymbol{u}, q) - 1/\lambda \; c(p, q) = \quad 0 \quad \forall q \in U, \end{cases}$$

where we denote with the same letters the bilinear forms obtained using the appropriate quadrature rule described above. In matrix form, we have

$$K \begin{bmatrix} \boldsymbol{u} \\ p \end{bmatrix} = \begin{bmatrix} A & B^T \\ B & -1/\lambda \; C \end{bmatrix} \begin{bmatrix} \boldsymbol{u} \\ p \end{bmatrix} = \begin{bmatrix} \boldsymbol{b} \\ 0 \end{bmatrix}.$$

4.2. *Substructuring for Saddle Point Problems*

The domain $\Omega = \bigcup_{i=1}^{N} \Omega_i \cup \Gamma$ is decomposed into open, nonoverlapping hexahedral (quadrilateral) subdomains Ω_i and the interface $\Gamma = \left(\bigcup_{i=1}^{N} \partial\Omega_i \right) \setminus \partial\Omega$. Each Ω_i typically consists of one, or a few, spectral elements of degree n or of many finite elements. We denote by Γ_h and $\partial\Omega_h$ the set of nodes belonging to the interface Γ and $\partial\Omega$, respectively. The starting point of our algorithm is the implicit elimination (static condensation) of the interior degrees of freedom (displacements supported in the open subdomains and interior pressures with zero average over the individual subdomains), by solving decoupled local saddle point problems on each Ω_i with Dirichlet boundary conditions for the displacements on $\partial\Omega_i$. We then obtain a saddle point Schur complement problem for the interface displacements and a constant pressure in each subdomain. This reduced problem will be solved by a preconditioned Krylov space iteration, normally the preconditioned conjugate gradient method. We reorder the vector of unknowns as

$$\begin{bmatrix} \boldsymbol{u}_I \\ p_I \\ \boldsymbol{u}_\Gamma \\ p_0 \end{bmatrix} \begin{array}{l} \text{interior displacements} \\ \text{interior pressures with zero average} \\ \text{interface displacements} \\ \text{constant pressures in each } \Omega_i. \end{array}$$

Using the same permutation, the discrete system matrix can be written as

$$\begin{bmatrix} K_{II} & K_{\Gamma I}^T \\ K_{\Gamma I} & K_{\Gamma\Gamma} \end{bmatrix} = \left[\begin{array}{cc|cc} A_{II} & B_{II}^T & A_{\Gamma I}^T & 0 \\ B_{II} & -1/\lambda\, C_{II} & B_{I\Gamma} & 0 \\ \hline A_{\Gamma I} & B_{I\Gamma}^T & A_{\Gamma\Gamma} & B_0^T \\ 0 & 0 & B_0 & 1/\lambda\, C_0 \end{array}\right].$$

Eliminating the interior unknowns $\boldsymbol{u}_I$ and p_I by static condensation, we obtain the saddle point Schur complement system

$$S_\lambda \begin{bmatrix} \boldsymbol{u}_\Gamma \\ p_0 \end{bmatrix} = \begin{bmatrix} \tilde{\boldsymbol{b}} \\ 0 \end{bmatrix}, \tag{8}$$

$$\text{where} \quad S_\lambda = K_{\Gamma\Gamma} - K_{\Gamma I} K_{II}^{-1} K_{\Gamma I}^T = \begin{bmatrix} S_{\Gamma,\lambda} & B_0^T \\ B_0 & -1/\lambda\, C_0 \end{bmatrix},$$

$$= \begin{bmatrix} A_{\Gamma\Gamma} & B_0^T \\ B_0 & -1/\lambda\, C_0 \end{bmatrix} - \begin{bmatrix} A_{\Gamma I} & B_{I\Gamma}^T \\ 0 & 0 \end{bmatrix} \begin{bmatrix} A_{II} & B_{II}^T \\ B_{II} & -1/\lambda\, C_{II} \end{bmatrix}^{-1} \begin{bmatrix} A_{\Gamma I}^T & 0 \\ B_{I\Gamma} & 0 \end{bmatrix},$$

$$\begin{bmatrix} \tilde{\boldsymbol{b}} \\ 0 \end{bmatrix} = \begin{bmatrix} \boldsymbol{b}_\Gamma \\ 0 \end{bmatrix} - \begin{bmatrix} A_{\Gamma I} & B_{I\Gamma}^T \\ 0 & 0 \end{bmatrix} \begin{bmatrix} A_{II} & B_{II}^T \\ B_{II} & -1/\lambda\, C_{II} \end{bmatrix}^{-1} \begin{bmatrix} \boldsymbol{b}_I \\ 0 \end{bmatrix}.$$

K_{II}^{-1} represents the solution of N decoupled saddle point problems, one for each subdomain and all uniquely solvable, with Dirichlet data given on $\partial\Omega_i$. The Schur complement S_λ does not need to be explicitly assembled since only its action $S_\lambda v$ on a vector v is needed in a Krylov iteration. This operation essentially only requires the action of K_{II}^{-1} on a vector, i.e., the solution of N decoupled saddle point problems. In other words, $S_\lambda v$ is computed by subassembling the actions of the local Schur complements $S_\lambda^{(i)} = K_{\Gamma\Gamma}^{(i)} - K_{\Gamma I}^{(i)} (K_{II}^{(i)})^{-1} K_{\Gamma I}^{(i)^T}$. This substructuring procedure is associated with the space decomposition

$$\boldsymbol{V} \times U = \bigoplus_{i=1}^{N} \boldsymbol{V}_i \times U_i \oplus \boldsymbol{V}_\Gamma \times U_0,$$

where the interior spaces are defined as $\boldsymbol{V}_i = \boldsymbol{V} \cap H_0^1(\Omega_i)$, $U_i = U \cap L_0^2(\Omega_i)$, and the spaces of interface displacements and coarse pressures, constant in each subdomain, are defined as

$$\boldsymbol{V}_\Gamma = \mathcal{SH}_\lambda(\boldsymbol{V}_{|\Gamma}) = \{\boldsymbol{v} \in \boldsymbol{V} : \boldsymbol{v}_{|\Omega_i} = \mathcal{SH}_\lambda(\boldsymbol{v}_{|\partial\Omega_i}),\ \ i = 1, \dots, N\},$$

$$U_0 = \{q \in U : q_{|\Omega_i} = \text{constant},\ \ i = 1, \dots, N\}.$$

Here $\mathcal{SH}_\lambda$: $\boldsymbol{V}_{|\Gamma} \to \boldsymbol{V}$, is the displacement component of the discrete saddle point harmonic extension operator that maps an interface displacement $\boldsymbol{u}_\Gamma \in \boldsymbol{V}_{|\Gamma}$ onto the solution $(\tilde{\boldsymbol{u}}, \tilde{p})^T$ of the following homogeneous saddle point problem, defined on each subdomain separately: find $\tilde{\boldsymbol{u}} \in \boldsymbol{V}$ and $\tilde{p} \in U$ such that on

each Ω_i,

$$\text{(9)} \qquad \begin{cases} a(\tilde{\boldsymbol{u}}, \boldsymbol{v}) + b(\boldsymbol{v}, \tilde{p}) = 0 \ \forall \boldsymbol{v} \in \boldsymbol{V}_i \\ b(\tilde{\boldsymbol{u}}, q) - 1/\lambda\, c(\tilde{p}, q) = 0 \ \forall q \in U_i \\ \tilde{\boldsymbol{u}} = \boldsymbol{u}_\Gamma \text{ on } \partial\Omega_i. \end{cases}$$

If we define the interface inner product by

$$s_\lambda(\boldsymbol{u}_\Gamma, \boldsymbol{v}_\Gamma) = a(\mathcal{SH}_\lambda(\boldsymbol{u}_\Gamma), \mathcal{SH}_\lambda(\boldsymbol{v}_\Gamma)) = \boldsymbol{u}_\Gamma^T S_{\Gamma,\lambda} \boldsymbol{v}_\Gamma,$$

and by $b_0(\boldsymbol{u}_\Gamma, p_0)$ and $c_0(p_0, q_0)$ the restrictions of the other bilinear forms to the saddle point harmonic extensions and the coarse piecewise constant pressures, then the variational formulation of the saddle point Schur complement problem (8) can be given by: find $\boldsymbol{u}_\Gamma \in \boldsymbol{V}_\Gamma$ and $p_0 \in U_0$ such that,

$$\text{(10)} \qquad \begin{cases} s_\lambda(\boldsymbol{u}_\Gamma, \boldsymbol{v}_\Gamma) + b_0(\boldsymbol{v}_\Gamma, p_0) = \tilde{\mathbf{F}}(\boldsymbol{v}_\Gamma) \ \forall \boldsymbol{v}_\Gamma \in \boldsymbol{V}_\Gamma \\ b_0(\boldsymbol{u}_\Gamma, q_0) - 1/\lambda\, c_0(p_0, q_0) = 0 \quad \forall q_0 \in U_0. \end{cases}$$

On the benign subspace $(\boldsymbol{V}_\Gamma \times U_0)_B$ defined by

$$(\boldsymbol{V}_\Gamma \times U_0)_B = \{(\boldsymbol{u}_\Gamma, p_0) \in \boldsymbol{V}_\Gamma \times U_0 \colon b_0(\boldsymbol{u}_\Gamma, q_0) - 1/\lambda\, c_0(p_0, q_0) = 0\},$$

problem (10) is equivalent to the positive definite problem: find $(\boldsymbol{u}_\Gamma, p_0) \in (\boldsymbol{V}_\Gamma \times U_0)_B$ such that

$$\text{(11)} \qquad s_\lambda(\boldsymbol{u}_\Gamma, \boldsymbol{v}_\Gamma) + 1/\lambda c_0(p_0, q_0) = \tilde{\boldsymbol{F}}(\boldsymbol{v}_\Gamma) \qquad \forall (\boldsymbol{v}_\Gamma, q_0) \in (\boldsymbol{V}_\Gamma \times U_0)_B.$$

4.3. *Neumann-Neumann Preconditioners.*

We will solve the saddle point Schur complement problem

$$\text{(12)} \qquad S_\lambda \begin{bmatrix} \boldsymbol{u}_\Gamma \\ p_0 \end{bmatrix} = \begin{bmatrix} S_{\Gamma,\lambda} & B_0^T \\ B_0 & -1/\lambda\, C_0 \end{bmatrix} \begin{bmatrix} \boldsymbol{u}_\Gamma \\ p_0 \end{bmatrix} = \begin{bmatrix} \tilde{\boldsymbol{b}} \\ 0 \end{bmatrix}$$

by a preconditioned Krylov space method such as GMRES or PCG. The matrix form of the preconditioner is

$$\text{(13)} \qquad Q_\lambda = Q_H + (I - Q_H S_\lambda) \sum_{i=1}^{N} Q_i (I - S_\lambda Q_H),$$

where the coarse operator Q_H and local operators Q_i are defined below. The preconditioned operator is then

$$\text{(14)} \qquad T_\lambda = Q_\lambda S_\lambda = T_0 + (I - T_0) \sum_{i=1}^{N} T_i (I - T_0),$$

where $T_0 = Q_H S_\lambda$ and $T_i = Q_i S_\lambda$. The balancing Neumann-Neumann precondi-

tioner T_λ is associated with further decomposing the interface space $\boldsymbol{V}_\Gamma \times U_0$ as

$$\boldsymbol{V}_\Gamma \times U_0 = \boldsymbol{V}_0 \times U_0 + \sum_{i=1}^{N} \boldsymbol{V}_{\Gamma_i} \times U_{0,i}.$$

Here, the coarse displacement space $\boldsymbol{V}_0$ is defined in terms of special functions $\delta_i^\dagger$ introduced below and is given by either one of the three following choices:

$$\boldsymbol{V}_0^0 = \{\boldsymbol{v} \in \boldsymbol{V}_\Gamma\colon \boldsymbol{v} \in span\,\{\delta_i^\dagger\} \ \textit{times the functions spanning} \ \ker(a)\},$$

$$\boldsymbol{V}_0^1 = \boldsymbol{V}_0^0 \cup span\,\{\textit{normal direction quadratic edge/face bubble functions}\},$$

$$\boldsymbol{V}_0^2 = \boldsymbol{V}_0^0 \cup span\,\{\textit{bi- or tri-linear coarse piecewise } Q_1 \textit{ functions}\},$$

while the local spaces are defined by:

$$\boldsymbol{V}_{\Gamma,i} = \{\boldsymbol{v} \in \boldsymbol{V}_\Gamma\colon \boldsymbol{v}(x) = 0 \ \ \forall x \in \Gamma_h \setminus \partial\Omega_{i,h}\}, \qquad U_{0,i} = span\,\{1\}.$$

We could also consider richer coarse spaces obtained, e.g., by adding to $\boldsymbol{V}_0^0$ functions of $\boldsymbol{V}_\Gamma$ that are piecewise tri- or bi-quadratic polynomials on Γ, as we did in our study [34] of the Stokes case.

4.3.1. Coarse problem. – Given a residual vector r, the coarse term $Q_H r$ is the solution of a coarse, global saddle point problem with a few displacement degrees of freedom and one constant pressure per subdomain Ω_i:

$$Q_H = R_H^T S_{0,\lambda}^{-1} R_H,$$

where

$$R_H = \begin{bmatrix} L_0^T & 0 \\ 0 & I \end{bmatrix}, \quad S_{0,\lambda} = R_H S_\lambda R_H^T = \begin{bmatrix} L_0^T S_{\Gamma,\lambda} L_0 & L_0^T B_0^T \\ B_0 L_0 & -1/\lambda\ C_0 \end{bmatrix}. \tag{15}$$

The columns of the matrix L_0 span the coarse space $\boldsymbol{V}_0$ and in order to define them, we need to define the Neumann-Neumann counting functions $\delta_i \in \boldsymbol{V}_\Gamma$ and their pseudo inverses $\delta_i^\dagger$ associated with each subdomain Ω_i: δ_i is zero at the interface nodes outside $\partial\Omega_{i,h}$ while its value at any node on $\partial\Omega_{i,h}$ equals the number of subdomains shared by that node; the pseudo inverse $\delta_i^\dagger$ is the function $1/\delta_i(x)$ for all nodes where $\delta_i(x) \neq 0$, and it vanishes at all other points of $\Gamma_h \cup \partial\Omega_h$. Then, the columns of L_0 are defined by one of the following three choices: ($\boldsymbol{V}_0^0$) the inverse counting functions $\delta_i^\dagger$ multiplied by the functions of $\ker(a)$; ($\boldsymbol{V}_0^1$) as in $\boldsymbol{V}_0^0$ with the addition of the quadratic coarse edge/face bubble functions for the normal direction; ($\boldsymbol{V}_0^2$) as in $\boldsymbol{V}_0^0$ with the addition of the continuous piecewise bi- or tri-linear functions on the coarse mesh τ_H. $\boldsymbol{V}_0^0$ corresponds to the standard choice for second order scalar elliptic pro-

blems and it provides a quite minimal coarse displacement space. It turns out to be far from uniformly inf-sup stable and therefore it leads to a nonscalable algorithm in the incompressible case. However, in the compressible case where λ/μ is bounded, it still leads to a scalable algorithm; see our main theorem and the numerical results. $\boldsymbol{V}_0^1$ and $\boldsymbol{V}_0^2$ are enrichments of $\boldsymbol{V}_0^0$ that turn out to be inf-sup stable uniformly in N and λ/μ.

4.3.2. Local problems. – Given a residual vector r with a first component r_Γ and a zero second component, $Q_i r$ is the weighted solution of a local saddle point problem on subdomain Ω_i with a natural boundary condition on $\partial\Omega_i \setminus \Gamma_0$:

$$Q_i r = \begin{bmatrix} R_i^T D_i^{-1} & 0 \\ 0 & 0 \end{bmatrix} \begin{bmatrix} S_{\Gamma,\varepsilon,\lambda}^{(i)} & B_0^{(i)T} \\ B_0^{(i)} & -1/\lambda\ C_0^{(i)} \end{bmatrix}^{-1} \begin{bmatrix} D_i^{-1} R_i & 0 \\ 0 & 0 \end{bmatrix} \begin{bmatrix} r_\Gamma \\ 0 \end{bmatrix}. \tag{16}$$

Here R_i are 0, 1 restriction matrices mapping r_Γ into r_{Γ_i} and D_i are diagonal matrices representing multiplication by the counting functions δ_i. Moreover,

$$S_\varepsilon^{(i)} = \begin{bmatrix} S_{\Gamma,\varepsilon,\lambda}^{(i)} & B_0^{(i)T} \\ B_0^{(i)} & -1/\lambda\ C_0^{(i)} \end{bmatrix}$$

is the local saddle point Schur complement, associated with the subdomain Ω_i, of the regularized local stiffness matrix

$$K_\varepsilon^{(i)} = \begin{bmatrix} A_{II,\varepsilon}^{(i)} & B_{II}^{(i)T} & A_{I\Gamma,\varepsilon}^{(i)T} & 0 \\ B_{II}^{(i)} & -1/\lambda\ C_{II}^{(i)} & B_{I\Gamma}^{(i)} & 0 \\ A_{I\Gamma,\varepsilon}^{(i)} & B_{I\Gamma}^{(i)T} & A_{\Gamma\Gamma,\varepsilon}^{(i)} & B_0^{(i)T} \\ 0 & 0 & B_0^{(i)} & -1/\lambda\ C_0^{(i)} \end{bmatrix},$$

where $A_\varepsilon^{(i)} = A^{(i)} + \varepsilon M^{(i)}$. Here $M^{(i)}$ is the local displacement mass matrix.

4.4. *Convergence rate analysis.*

The following result has been proven in [34] for the Stokes case and in [20] for the elasticity case.

THEOREM 4. – *On the benign subspace* $(\boldsymbol{V}_\Gamma \times U_0)_B$ *the balancing Neumann-Neumann operator* T_λ *is symmetric, positive definite with respect to the* λ*-inner product*

$$\left\langle \begin{bmatrix} \boldsymbol{u}_\Gamma \\ p_0 \end{bmatrix}, \begin{bmatrix} \boldsymbol{v}_\Gamma \\ q_0 \end{bmatrix} \right\rangle_\lambda = s_\lambda(\boldsymbol{u}_\Gamma, \boldsymbol{v}_\Gamma) + 1/\lambda\ c_0(p_0, q_0),$$

and its condition number is bounded by

$$cond\,(T_\lambda) \leqslant C\left(2+\frac{\sqrt{d/2}}{\sqrt{\beta_0^2+\mu/\lambda}}\right)\left(1+\frac{\sqrt{d}}{\sqrt{\beta^2+\mu/\lambda}}\right)^2\alpha\,,$$

where

$$\alpha=\begin{cases}(1+\log(H/h))^2 & \text{for finite elements}\\ (1+\log n)^2 & \text{for spectral elements},\end{cases}$$

and β_0 and β are the inf-sup constants of the coarse problem and the original discrete saddle point problem, respectively. The constant C in the bound is uniform in the parameter ε used in the regularization of the local Neumann problems.

4.5. *Variable Coefficient and Composite Materials.*

Our algorithm can be extended to composite materials with different Lamé constants λ_i, μ_i in each subdomain Ω_i:

$$(17)\qquad \begin{cases} 2\sum_{i=1}^{N}\int_{\Omega_i}\mu_i\,\varepsilon(\boldsymbol{u}):\varepsilon(\boldsymbol{v})\,dx \;-\; \int_{\Omega}\operatorname{div}\boldsymbol{v}\,p\,dx \;=\; \langle \boldsymbol{F},\,\boldsymbol{v}\rangle \;\;\forall \boldsymbol{v}\in\widetilde{\boldsymbol{V}} \\ -\int_{\Omega}\operatorname{div}\boldsymbol{u}\,q\,dx \;-\; \sum_{i=1}^{N}\int_{\Omega_i}1/\lambda_i\,pq\,dx \;=\; 0 \qquad \forall q\in\widetilde{U}\,; \end{cases}$$

Using the convention of padding local vectors by zeros, when they are needed as global vectors, the discrete problem can now be written as

$$K\begin{bmatrix}\boldsymbol{u}\\ p\end{bmatrix}=\sum_{i=1}^{N}\begin{bmatrix}A^{(i)} & B^{(i)^T}\\ B^{(i)} & -1/\lambda_i\;C^{(i)}\end{bmatrix}\begin{bmatrix}\boldsymbol{u}^{(i)}\\ p^{(i)}\end{bmatrix},$$

and the saddle point Schur complement obtained by static condensation as

$$S\begin{bmatrix}\boldsymbol{u}_\Gamma\\ p_0\end{bmatrix}=\sum_{i=1}^{N}\begin{bmatrix}S_\Gamma^{(i)} & B_0^{(i)^T}\\ B_0^{(i)} & -1/\lambda_i\;C_0^{(i)}\end{bmatrix}\begin{bmatrix}\boldsymbol{u}_\Gamma^{(i)}\\ p_0^{(i)}\end{bmatrix}.$$

The balancing Neumann-Neumann preconditioner Q for S has the same matrix form as before, but with modified local and coarse spaces. As in the scalar elliptic case, the jumps in the coefficients μ_i are taken care of by appropriately scaling the special counting functions δ_i and their pseudo inverses $\delta_i^\dagger$. At any node x on $\partial\Omega_i$, we use the definition:

$$\delta_i^\dagger(x)=\frac{\mu_i^\gamma(x)}{\sum_{j\in N_x}\mu_j^\gamma(x)}\,,$$

where $\gamma \in [1/2, \infty)$ and N_x is the set of indices of all the subdomains that have x on their boundaries. Both functions δ_i and $\delta_i^\dagger$ vanish at each interface node outside $\partial\Omega_{i,h}$ and are extended inside each subdomain as discrete saddle point harmonic extensions; they still form a partition of unity. The local and coarse problems are then defined formally as before but using these modified functions δ_i and $\delta_i^\dagger$.

4.6. *Numerical experiments.*

In this section, we report on numerical results for the Stokes and almost incompressible elasticity systems. We show first some results of parallel numerical experiments on the Beowulf cluster Chiba City at Argonne National Laboratory (with 256 Dual Pentium III processors). The algorithm has been implemented by Paulo Goldfeld in C, using the PETSc library; see [7, 8]. The problem is discretized with $Q_2 - Q_0$ finite elements and the domain Ω is the unit square divided into $\sqrt{N} \times \sqrt{N}$ square subdomains. The saddle point Schur complement (12) is solved iteratively by PCG with our balancing Neumann-Neumann preconditioner and the third choice of coarse space $V_0^2 = \{\text{scaled rigid body motions}\} + Q_1^H$. The initial guess is a random vector modified so that the initial error is in the range of $(I - T_0)$, the right hand side is a random, uniformly distributed vector projected onto the range of S, and the stopping criterion is $\|r_k\|_2/\|r_0\|_2 \leq 10^{-6}$, where r_k is the residual at the k-th iterate.

4.6.1. Stokes problem on a homogeneous medium. – We consider first the incompressible Stokes problem with constant coefficients and in the upper half of Table 1, we show the results for increasing mesh sizes, always partitio-

TABLE 1. – *Parallel results for Stokes system (homogeneous medium) and $Q_2 - Q_0$ finite elements: PCG iteration counts and extremal eigenvalues of T_λ for the balancing Neumann-Neumann preconditioner with coarse space V_0^2.*

Fixed number of subdomains $N = 8 \times 8$					
mesh size	local size	# unknowns	iterations	eig min	eig max
160×160	20×20	231,683	18	1.06	8.31
320×320	40×40	924,163	21	1.07	11.08
480×480	60×60	2,077,443	22	1.07	12.89
Fixed local size 60×60 elements (32,883 unknowns)					
mesh size	# subdomains	# unknowns	iterations	eig min	eig max
240×240	4×4	520,323	20	1.07	11.36
360×360	6×6	1,169,283	22	1.07	12.43
480×480	8×8	2,077,443	22	1.07	12.89
720×720	12×12	4,671,363	23	1.07	13.32
840×840	14×14	6,357,123	23	1.07	13.44

ned into 64 subdomains. The lower part of Table 1 shows results for an increasing number of subdomains of a fixed size. These results agree with the theory, since in the finite element case we have inf-sup stability of both the original and coarse problems and therefore both inf-sup constants β and β_0 are bounded away from zero independently of h and H.

4.6.2. Elasticity problem on a heterogeneous medium. – Here we consider an elasticity problem defined in a heterogeneous medium, which is composed of an arrangement of three different materials in the following pattern, where s = steel-like ($\mu_s = 8.20$, $\lambda_s = 10.00$, $\nu_s = 0.275$), a = aluminium-like ($\mu_a = 2.60$, $\lambda_a = 5.60$, $\nu_a = 0.341$), r = rubber-like ($\mu_r = 0.01$, $\lambda_r = 0.99$, $\nu_r = 0.495$):

s	r	s	r	$\cdots$	s	r
r	a	r	a	$\cdots$	r	a
s	r	s	r	$\cdots$	s	r
r	a	r	a	$\cdots$	r	a
$\vdots$	$\vdots$	$\vdots$	$\vdots$	$\ddots$	$\vdots$	$\vdots$
s	r	s	r	$\cdots$	s	r
r	a	r	a	$\cdots$	r	a

,

Note that the material r is almost incompressible, with a Poisson ratio close to 0.5. As in the previous example, we show, in the upper half of Table 2, the results for meshes of increasing sizes partitioned into 64 subdomains. Again, the condition number and the iteration count grow slowly with the size of the local problem, as in the homogeneous case. The last two columns of this table display CPU-time for these runs. The last column gives the total time for the code to run, while the column labeled «fact.» gives the time spent on LU factorizations (a Dirichlet and a Neumann problem on each subdomain and one global coarse problem). The lower part of Table 2 shows results for an increasing number of subdomains of fixed size (about 58 thousand dofs). Again, we observe no influence of the number of subdomains on the condition number or iteration count. This shows that our main result on Section 4 remains valid in the case of discontinuous coefficients.

4.6.3. Serial results for $Q_n - Q_{n-2}$ Spectral Elements. – We next consider the case of a heterogeneous material occupying a cubic domain Ω. The problem is discretized with $Q_n - Q_{n-2}$ spectral elements and the algorithm was implemented in Matlab on a Unix workstation. Figure 1 shows the distribution

TABLE 2. – *Parallel results for linear elasticity system (heterogeneous medium) and $Q_2 - Q_0$ finite elements: PCG iteration counts and extremal eigenvalues of T_λ for the balancing Neumann-Neumann preconditioner with coarse space V_0^2.*

Fixed number of subdomains $N = 8 \times 8$

					CPU time (sec.)	
mesh size	local size	# unkn.	iter.	eig max	fact.	total
160×160	20×20	230,000	12	4.06	1.4	18.0
320×320	40×40	920,000	13	4.65	18.2	40.9
480×480	60×60	2,080,000	14	4.99	84.2	126.3
640×640	80×80	3,690,000	14	5.22	260.8	345.3

Fixed local size 80×80 elements (58,242 unknowns)

					CPU time (sec.)	
mesh size	# subdom.	# unkn.	iter.	eig max	fact.	total
320×320	4×4	920,000	12	5,18	258.0	321.4
480×480	6×6	2,080,000	13	5.21	253.7	317.4
640×640	8×8	3,690,000	14	5.22	260.8	345.3
800×800	10×10	5,770,000	14	5.14	262.8	356.7
1040×1040	13×13	9,740,000	14	4.93	261.2	363.9

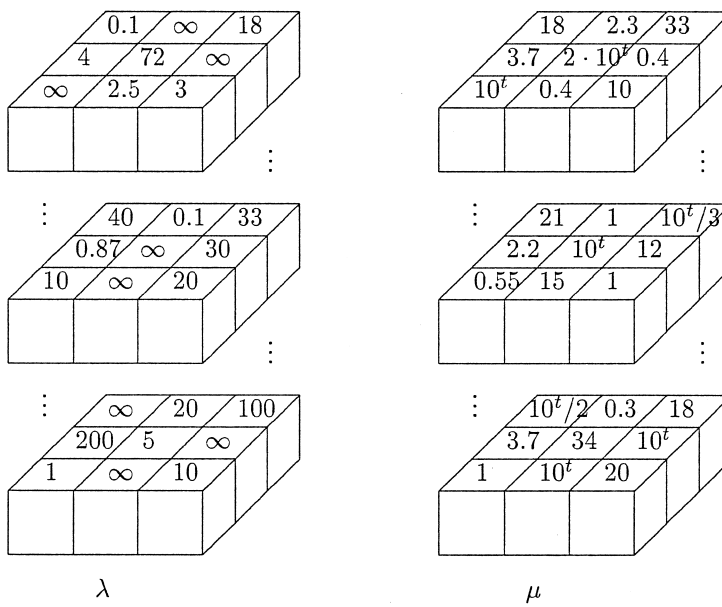

Fig. 1. – 3D results: Distribution of the Lamé coefficients λ (left) and μ (right) on horizontal sections of a cubic domain.

TABLE 3. – *Serial results in 3D for elasticity system (heterogeneous medium) and spectral elements: PCG iteration counts and maximum eigenvalue of T_λ for the balancing Neumann-Neumann preconditioner. Fixed number of subdomains $N = 3 \times 3$ and spectral degree $n = 4$.*

	V_0^0 coarse space		
exponent t in μ	# iterations	eig max	eig min
-3	18	6.68	1.0003
-1	16	6.43	1.0039
0	15	5.16	1.0049
1	17	6.39	1.0048
3	19	7.52	1.0029
6	19	7.59	1.0030

of the Lamé coefficients λ (left) and μ (right) on a cubic domain; the exponent t ranges from $t = -3$ to $t = 6$ and there are incompressible subdomains. The results reported in Table 3 show that also in three dimensions the performance of our algorithm and the spectrum of the preconditioned operator are independent of the jumps in the Lamé coefficients.

5. – Application 2: Block Jacobi preconditioners for reaction-diffusion systems in electrocardiology.

We now present a second application of domain decomposition methods to reaction-diffusion systems arising in computational electrocardiology; more details can be found in Colli Franzone and Pavarino [14]. These models describe the electrical potentials involved in the excitation of the cardiac muscle and in recent years have been subject to intense interdisciplinary studies bridging medicine, bioengineering and scientific computing; see e.g. [1, 2, 3, 19, 42].

5.1. *The cardiac Bidomain and Monodomain models.*

Cardiac tissue is traditionally modeled as an arrangement of cardiac fibers that rotate counterclockwise from the epicardium to the endocardium, (the outer and inner boundaries of the cardiac muscle). Moreover, the cardiac tissue has a laminar organization that can be modeled as a set of muscle sheets running radially from epi to endocardium. Therefore, at any point $\boldsymbol{x}$, it is possible to identify a triplet of orthonormal principal axes $\boldsymbol{a}_l(\boldsymbol{x})$, $\boldsymbol{a}_t(\boldsymbol{x})$, $\boldsymbol{a}_n(\boldsymbol{x})$, with $\boldsymbol{a}_l(\boldsymbol{x})$ parallel to the local fiber direction, $\boldsymbol{a}_t(\boldsymbol{x})$ and $\boldsymbol{a}_n(\boldsymbol{x})$ tangent and orthogonal to the radial laminae respectively and both being transversal to the fiber axis. The macroscopic Bidomain model represents the cardiac tissue as the superposition of two anisotropic continuous media, the intra (i) and extra (e) cellular

media, coexisting at every point of the tissue and connected by a distributed continuous cellular membrane; see Keener and Sneyd [22]. The anisotropic conductivity properties of the tissue are described by the conductivity coefficients in the intra and extracellular media $\sigma_l^{i,e}$, $\sigma_t^{i,e}$, $\sigma_n^{i,e}$, measured along the corresponding directions $\boldsymbol{a}_l$, $\boldsymbol{a}_t$, $\boldsymbol{a}_n$, and by the conductivity tensors $D_i(\boldsymbol{x})$ and $D_e(\boldsymbol{x})$

$$D_{i,e} = \sigma_l^{i,e}\ \boldsymbol{a}_l\boldsymbol{a}_l^T + \sigma_t^{i,e}\ \boldsymbol{a}_t\boldsymbol{a}_t^T + \sigma_n^{i,e}\ \boldsymbol{a}_n\boldsymbol{a}_n^T.$$

When the media are *axially isotropic*, i.e. when $\sigma_n^{i,e} = \sigma_t^{i,e}$, we have $D_{i,e} = \sigma_t^{i,e} I + (\sigma_l^{i,e} - \sigma_t^{i,e})\,\boldsymbol{a}_l\boldsymbol{a}_l^T$. The intra and extracellular electric potentials u_i, u_e in an insulated cardiac domain H are described in the Bidomain model by a reaction-diffusion system coupled with a system of ODEs for the ionic gating variables w. Given the applied currents per unit volume $I_{\text{app}}^{i,e}$, satisfying the compatibility condition $\int_H I_{\text{app}}^i \,\mathrm{dx} = \int_H I_{\text{app}}^e \,\mathrm{dx}$, the initial conditions v_0, w_0, then u_i, u_e, w satisfy the system:

$$\text{(18)}\qquad \begin{cases} c_m \dfrac{\partial v}{\partial t} - div\,(D_i \nabla u_i) + I_{\text{ion}}(v, w) = I_{\text{app}}^i \\ -c_m \dfrac{\partial v}{\partial t} - div(D_e \nabla u_e) - I_{\text{ion}}(v, w) = -I_{\text{app}}^e \\ \dfrac{\partial w}{\partial t} - R(v, w) = 0, \ v(t) = u_i(t) - u_e(t) \\ \boldsymbol{n}^T D_i \nabla u_i = 0, \quad \boldsymbol{n}^T D_e \nabla u_e = 0, \\ v(\boldsymbol{x}, 0) = v_0(\boldsymbol{x}), \quad w(\boldsymbol{x}, 0) = w_0(\boldsymbol{x}), \end{cases}$$

where $c_m = \chi * C_m$, $I_{\text{ion}} = \chi * i_{\text{ion}}$, with χ the ratio of membrane surface area per tissue volume, C_m the membrane capacitance and i_{ion} the ionic current of the membrane per unit area. Existence and regularity results for this degenerate system can be found in Colli Franzone and Savarè [15]. The system uniquely determines v, while the potentials u_i and u_e are defined only up to a same additive time-dependent constant related to the reference potential, chosen to be the average extracellular potential in the cardiac volume by imposing $\int_H u_e \,\mathrm{dx} = 0$.

If the two media have equal anisotropy ratio, i.e. $D_i = \lambda D_e$ with λ constant, then the Bidomain system reduces to the Monodomain model consisting in a parabolic reaction-diffusion equation for the transmembrane potential v cou-

pled with a system of ODEs for the gating variables:

$$
(19)\qquad \begin{cases} c_m \dfrac{\partial v}{\partial t} - div(D_m(\boldsymbol{x})\,\nabla v) + I_{\text{ion}}(v,\, w) = I^m_{\text{app}}, \\ \dfrac{\partial w}{\partial t} - R(v,\, w) = 0,\ \ w(\boldsymbol{x},\, 0) = w_0(\boldsymbol{x}), \\ \boldsymbol{n}^T D_m \nabla v = 0,\ \ v(\boldsymbol{x},\, 0) = v_0(\boldsymbol{x}), \end{cases}
$$

where $D_m = \sigma_l \boldsymbol{a}_l \boldsymbol{a}_l^T + \sigma_t \boldsymbol{a}_t \boldsymbol{a}_t^T + \sigma_n \boldsymbol{a}_n \boldsymbol{a}_n^T$, with $\sigma_{l,t,n} = \lambda \sigma^i_{l,t,n}/(1+\lambda)$ and $I^m_{\text{app}} = (\lambda I^i_{\text{app}} + I^e_{\text{app}})/(1+\lambda)$.

The dynamics of S gating variables are described by a so-called membrane model, consisting of ordinary differential equations of the form

$$
(20)\qquad \frac{\partial w_j}{\partial t} = R_j(v,\, w_j) = (w_{j\infty}(v) - w_j)/\tau_j(v), \qquad j = 1, \ldots, S.
$$

In this paper, we consider one of the most used detailed membrane models in the literature, the Luo-Rudy phase I (LR1) model (see Luo and Rudy [27]), based on six gating variables and one variable for the calcium ionic concentration.

5.2. *Finite element space discretization.*

The Monodomain (19) and Bidomain models (18) are discretized by meshing the cardiac tissue volume Ω with a structured grid of hexahedral isoparametric Q_1 elements and by introducing the associated finite element space V_h. A semidiscrete problem is obtained by applying a standard Galerkin procedure and choosing a finite element basis $\{\phi_i\}$ for V_h. We denote by $\mathrm{M} = \{\mathrm{m}_{rs} = \int_\Omega \varphi_r \varphi_s \,\mathrm{dx}\}$ the symmetric mass matrix, by $\mathrm{A}_{m,i,e} = \{\mathrm{a}^{m,i,e}_{rs} = \int_\Omega (\nabla\varphi_r)^T D_{m,i,e}\, \nabla\varphi_s \,\mathrm{dx}\}$ the symmetric stiffness matrices and by $\mathrm{I}^h_{\text{ion}}$, $\mathrm{I}^{(m,i,e),h}_{\text{app}}$ the finite element interpolants of I_{ion} and $I^{m,i,e}_{\text{app}}$, respectively. Integrals are computed with a 3D trapezoidal quadrature rule, so the mass matrix M is lumped to diagonal form; see Quarteroni and Valli [35] for an introduction to finite element methods. For adaptive discretization methods see Moore [29] and Yu [43]. In our implementation, we have actually reordered the unknowns writing for every node the $\boldsymbol{u}_i$ and $\boldsymbol{u}_e$ components consecutively, so as to minimize bandwidth of the stiffness matrix.

5.3. *Semi-implicit time discretization.*

The time discretization is performed by a semi-implicit method using for the diffusion term the implicit Euler method, while the nonlinear reaction term I_{ion} is treated explicitly; see Ascher et al. [5]. The use of an implicit treat-

ment of the diffusion terms appearing in the Mono or Bidomain models is essential to allow an adaptive change of the time step according to the stiffness of the various phases of the heartbeat. The ODE system for the gating variables is discretized by the semi-implicit Euler method; in this way we decouple the gating variables by solving the gating system first (given the potential $\boldsymbol{v}^n$ at the previous time-step)

$$(\boldsymbol{w}^{n+1} - \boldsymbol{w}^n)/\Delta t = R(\boldsymbol{v}^n, \boldsymbol{w}^{n+1})$$

and then solving for $\boldsymbol{u}_i^{n+1}$, $\boldsymbol{u}_e^{n+1}$ in the *Bidomain case*

$$\left(\frac{c_m}{\Delta t}\begin{bmatrix} \mathrm{M} & -\mathrm{M} \\ -\mathrm{M} & \mathrm{M} \end{bmatrix} + \begin{bmatrix} \mathrm{A}_i & 0 \\ 0 & \mathrm{A}_e \end{bmatrix}\right)\begin{bmatrix} \boldsymbol{u}_i^{n+1} \\ \boldsymbol{u}_e^{n+1} \end{bmatrix} = \tag{21}$$

$$\frac{c_m}{\Delta t}\begin{bmatrix} \mathrm{M}(\ \boldsymbol{u}_i^n - \boldsymbol{u}_e^n) \\ \mathrm{M}[-\boldsymbol{u}_i^n + \boldsymbol{u}_e^n] \end{bmatrix} + \begin{bmatrix} \mathrm{M}[-\mathrm{I}_{\mathrm{ion}}^h(\boldsymbol{v}^n, \boldsymbol{w}^{n+1}) + \mathrm{I}_{\mathrm{app}}^{i,h}] \\ \mathrm{M}[\ \mathrm{I}_{\mathrm{ion}}^h(\boldsymbol{v}^n, \boldsymbol{w}^{n+1}) - \mathrm{I}_{\mathrm{app}}^{e,h}] \end{bmatrix},$$

where $\boldsymbol{v}^n = \boldsymbol{u}_i^n - \boldsymbol{u}_e^n$. As in the continuous model, $\boldsymbol{v}^n$ is uniquely determined, while $\boldsymbol{u}_i^n$ and $\boldsymbol{u}_e^n$ are determined only up to the same additive time-dependent constant chosen by imposing the condition $\mathbf{1}^T \mathrm{M} \boldsymbol{u}_e^n = 0$.

In the *Monodomain case*, we have to solve for $\boldsymbol{v}^{n+1}$

$$\left(\frac{c_m}{\Delta t}\mathrm{M} + \mathrm{A}_m\right)\boldsymbol{v}^{n+1} = \frac{c_m}{\Delta t}\mathrm{M}\boldsymbol{v}^n - \mathrm{M}\mathrm{I}_{\mathrm{ion}}^h(\boldsymbol{v}^n, \boldsymbol{w}^{n+1}) + \mathrm{M}\mathrm{I}_{\mathrm{app}}^{m,h}. \tag{22}$$

We employed an adaptive time-stepping strategy based on controlling the transmembrane potential variation $\Delta v = max(\boldsymbol{v}^{n+1} - \boldsymbol{v}^n)$ at each time-step, see Luo and Rudy [27]. If $\Delta v < \Delta v_{\min} = 0.05$ then we select $\Delta t = (\Delta v_{\max}/\Delta v)\Delta t$ (if smaller than $\Delta t_{\max} = 6$ msec), if $\Delta v > \Delta v_{\max} = 0.5$ then we select $dt = (\Delta v_{\min}/\Delta v)\, dt$ (if greater than $\Delta t_{\min} = 0.005$ msec). In order to guarantee a control on the variation of the gating variables of the LR1 membrane model as well, each gating equation of the system (20) is integrated exactly, while the calcium ionic concentration is updated using the explicit Euler method.

5.4. *A parallel solver with block Jacobi preconditioner.*

The linear system at each time step in the discrete problems is solved iteratively by the preconditioned conjugate gradient (PCG) method, using as initial guess the solution at the previous time step. The preconditioner used is a one-level block Jacobi preconditioner, where the blocks are associated with a partition of the degrees of freedom (domain) into disjoint blocks (subdomains). Using the notation of the abstract Schwarz theory of Section 3, this is a one-le-

TABLE 4. – *Parameters calibration for numerical tests.*

ellipsoidal geometry	$a_1 = b_1 = 1.5\ cm, \quad a_2 = b_2 = 2.7\ cm, \quad c_1 = 4.4, \quad c_2 = 5\ cm$ $\phi_{\min} = 0, \quad \phi_{\max} = 2\pi, \quad \theta_{\min} = -3\pi/8, \quad \theta_{\max} = \pi/8$
	$\chi = 10^3\, cm^{-1}, \quad C_m = 10^{-3}\, mF/cm^2$
Monodomain parameters	$\sigma_l = 1.2 \cdot 10^{-3}\, \Omega^{-1} cm^{-1}, \ \sigma_t = 2.5562 \cdot 10^{-4}\, \Omega^{-1} cm^{-1}$ $G = 1.5\ \Omega^{-1} cm^{-2}, \quad v_{th} = 13\ mV, \quad v_p = 100\ mV$ $\eta_1 = 4.4\ \Omega^{-1} cm^{-2}, \quad \eta_2 = 0.012, \quad \eta_3 = 1$
Bidomain parameters	$\sigma_l^e = 2 \cdot 10^{-3}\, \Omega^{-1} cm^{-1}, \quad \sigma_l^i = 3 \cdot 10^{-3}\, \Omega^{-1} cm^{-1}$ $\sigma_t^e = 1.3514 \cdot 10^{-3}\, \Omega^{-1} cm^{-1}, \quad \sigma_t^i = 3.1525 \cdot 10^{-4}\, \Omega^{-1} cm^{-1}$ $\sigma_n^e = \sigma_t^e/\mu_1, \quad \sigma_n^i = \sigma_t^i/\mu_2$ $\mu_1 = \mu_2 = 1$ axial isotropic case, $\mu_1 = 2, \mu_2 = 10$ orthotropic case

vel additive Schwarz preconditioner (without coarse term)

$$B_A^{-1} = \sum_{i=1}^{N} R_i^T A_i^{-1} R_i$$

defined by a decomposition of the finite element space $V = V_h$ into a direct sum of local subspaces

$$V = R_1^T V_1 + \ldots + R_N^T V_N.$$

Each subspace is spanned by the degrees of freedom of the associated block. As before, the local solvers are defined by $A_i = R_i A R_i^T$, where now

$$A = \frac{c_m}{\Delta t} \mathrm{M} + \mathrm{A}_m \quad \text{or} \quad A = \frac{c_m}{\Delta t} \begin{bmatrix} \mathrm{M} & -\mathrm{M} \\ -\mathrm{M} & \mathrm{M} \end{bmatrix} + \begin{bmatrix} \mathrm{A}_i & 0 \\ 0 & \mathrm{A}_e \end{bmatrix}$$

is the iteration matrix of the Monodomain or Bidomain model, respectively. Parallelization and portability are realized using the PETSc parallel library [7, 8], assigning each subdomain and the relative block to a different processor. We use ILU(0) solver on each block, the default choice in the PETSc library. The numerical experiments reported in the next section show that this block Jacobi preconditioner performs well in the Monodomain case, but not in the Bidomain case. Therefore, more research is needed in order to build better preconditioners, particularly with two or more levels; see Smith, Bjo.024rstad and Gropp [38].

5.5. *Numerical results.*

We have conducted several numerical experiments in three dimensions on distributed memory parallel architectures, with both the Monodomain and the Bidomain model coupled with the LR1 membrane model. The parallel machines employed are an IBM SP RS/6000 with 512 processors Power 4 of the Ci-

neca Consortium (www.cineca.it), an HP SuperDome 64000 with 64 processors PA8700 of the Cilea Consortium (www.cilea.it) and an IBM Linux Cluster with 52 Xeon processors at our Department (www.mat.unimi.it). We refer to [14] for more detailed numerical results.

5.5.1. Scaled speedup for Monodomain and Bidomain - LR1 models. – We consider first the Monodomain equation with LR1 ionic model, simulating on the IBM SP4 machine the initial depolarization of some ellipsoidal blocks after one stimulus of 250 mA/cm^3 has been applied for 1 msec on a small area (5 mesh points in each direction) of the epicardium. The blocks are chosen in increasing sizes so as to keep constant the number of mesh points per subdomain (processor). As shown in Figure 2, the domain varies from the smaller block with 8 subdomains to half ventricle with 128 subdomains. We fixed the local mesh in each subdomain to be of $75 \times 75 \times 50$ nodes (281,750 unknowns), hence varying the global number of unknowns of the linear system from $2.25 \cdot 10^6$ in the smaller case with 8 subdomains on a global mesh of $150 \times 150 \times 100$ nodes to $3.6 \cdot 10^7$ in the larger case with 128 subdomains on a global mesh of $600 \times 600 \times 100$ nodes. The model is run for 30 time steps of 0.05 msec each. At each time step, we compute the potential v, the gating and concentration variables $w_1, \ldots, w_7$ and the depolarization time. The results are reported in the upper part of Table 5. The assembling time, average number of PCG iterations per time step and the average time per time step (last three columns) are reasonably small. Up to 64 processors, the algorithm seems practically scalable, and even for 128 processors, the number of PCG iterations grows to just 8. We then consider the Bidomain system with LR1 ionic model, in the same setting (initial stimulus and domain decomposition) of the previous case. At each time step, we now compute the potentials u_i, u_e, the gating and concentration variables and the depolarization time. Due to the larger memory requirements of the Bidomain model, we used a smaller mesh of $50 \times 50 \times 35$ nodes in each subdomain (processor), hence varying the global number of unknowns of the linear system from $1.4 \cdot 10^6$ in the smaller case with 8 subdomains on a global

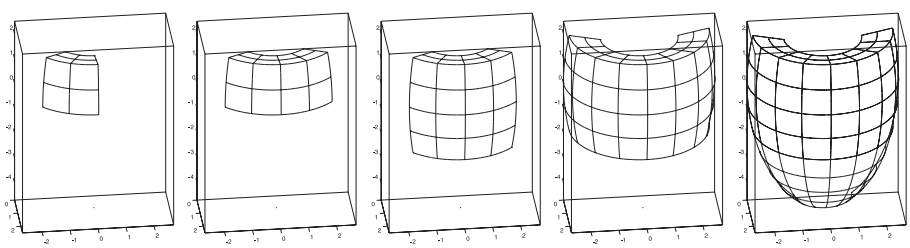

Fig. 2. – Scaled speedup test: ellipsoidal domains of increasing sizes decomposed into 8, 16, 32, 64 and 128 subdomains of fixed size.

TABLE 5. – *Scaled speedup tests for Monodomain - LR1 and Bidomain - LR1 models. Initial depolarization of an ellipsoidal block: 1 stimulus on epicardial surface,* 30 *time steps of* 0.05 *msec each, computation of* v, $w_1, \dots, w_7$ *and isochrones.* t_A = *assembly timing, it = average number of PCG iterations at each time step, time = average CPU timing of each time step.*

Monodomain - LR1					
# proc.	mesh	unknowns (nodes)	t_A	it.	time
$8 = 2 \cdot 2 \cdot 2$	$150 \cdot 150 \cdot 100$	2,250,000	7.7 s	4	2.7 s
$16 = 4 \cdot 2 \cdot 2$	$300 \cdot 150 \cdot 100$	4,500,000	8.5 s	4	3 s
$32 = 4 \cdot 4 \cdot 2$	$300 \cdot 300 \cdot 100$	9,000,000	9.1 s	5	3.6 s
$64 = 8 \cdot 4 \cdot 2$	$600 \cdot 300 \cdot 100$	18,000,000	9.2 s	5	3.6 s
$128 = 8 \cdot 8 \cdot 2$	$600 \cdot 600 \cdot 100$	36,000,000	10.6 s	8	5.1 s
Bidomain - LR1					
# proc.	mesh	unknowns ($2 \times$ nodes)	t_A	it.	time
$8 = 2 \cdot 2 \cdot 2$	$100 \cdot 100 \cdot 70$	1,400,000	12.9 s	98	40.2 s
$16 = 4 \cdot 2 \cdot 2$	$200 \cdot 100 \cdot 70$	12,800,000	13.3 s	127	55.5 s
$32 = 4 \cdot 4 \cdot 2$	$200 \cdot 200 \cdot 70$	5,600,600	15.7 s	148	72 s
$64 = 8 \cdot 4 \cdot 2$	$400 \cdot 200 \cdot 70$	11,200,000	16.2 s	176	91.9 s
$128 = 8 \cdot 8 \cdot 2$	$400 \cdot 400 \cdot 70$	22,400,000	18.4 s	244	129.7 s

mesh of $100 \times 100 \times 70$ to $2.24 \cdot 10^7$ unknowns in the larger case with 128 subdomains on a global mesh of $400 \times 400 \times 70$ nodes. The results are reported in the lower part of Table 5. While the assembling time remains reasonable (under 20 sec.), the average number of PCG iterations per time step and the average time per time step are now much larger, clearly showing the limits of the one-level preconditioner and the effects of the severe ill-conditioning of the Bidomain iteration matrix.

5.5.2. Simulation of a full cardiac cycle. – We simulated a complete cardiac cycle (excitation-recovery) with the Monodomain - LR1 model in a slab of cardiac tissue of size $5 \times 5 \times 1 \ cm^3$, with fibers that rotate linearly of 120^o intramurally and with initial stimulus at the center of the epicardium. The mesh was $501 \times 501 \times 101$, for a total of 25,351,101 nodes, while the simulated time was 550 msec., using about 3300 time steps of variable size. This simulation used 52 processors of our Linux Cluster for about 8.3 hours, averaging about 9 sec per time step. Figure 3 shows the isochrone lines of the activation time (ACTI), repolarization time (REPO) and their difference known as action potential duration (APD = REPO - ACTI) on the entire slab (lower row) and

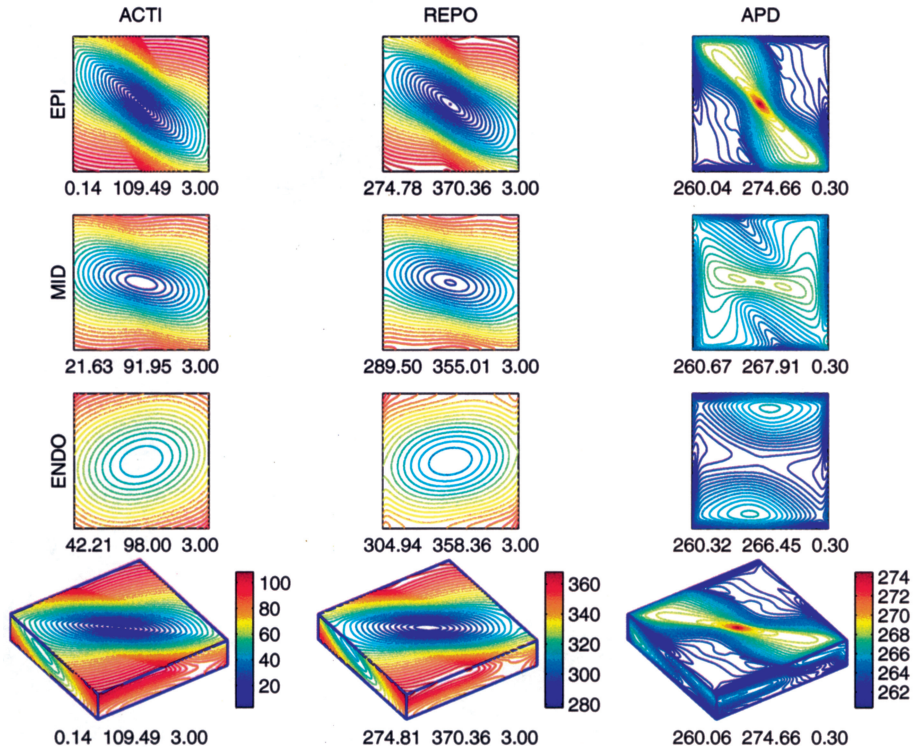

Fig. 3. – Simulation of full cardiac cycle. Isochrone lines of the activation time (ACTI), repolarization time (REPO) and action potential duration (APD = REPO - ACTI) on a slab $5 \times 5 \times 1$ cm^3 (lower row) and three horizontal sections corresponding to the epicardium (first row), midwall (second row) and endocardium (third row). Under each panel are reported the minimum and maximum value plotted and the step size between contour lines.

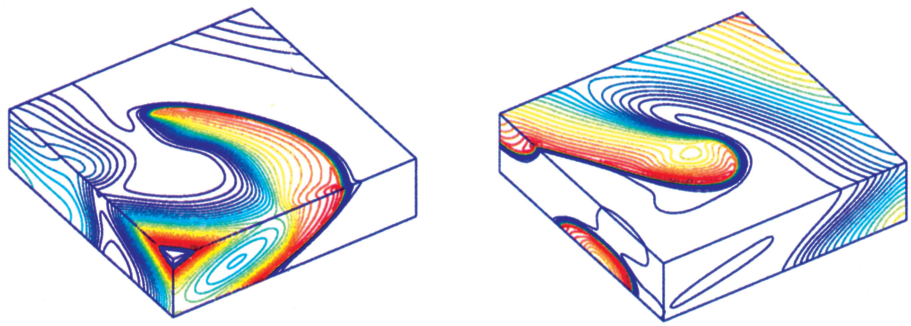

Fig. 4. – Stable spiral reentry with Bidomain - LR1 model on a domain $2 \times 2 \times 0.5$ cm^3. Plots show the potential v at times T = 150 and 190 msec. Colors range from blue (resting potential $= -84$ mV) to red (excitation wavefront).

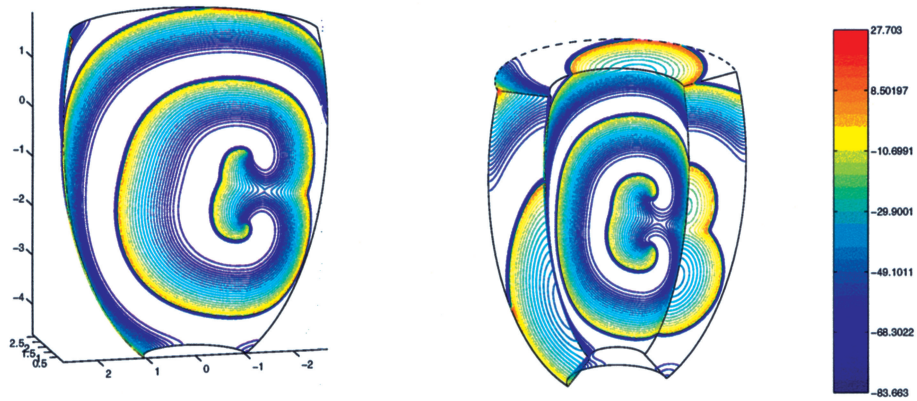

Fig. 5. – Stable double spiral reentry with Monodomain - LR1 model on an ellipsoidal domain discretized with a mesh $501 \times 501 \times 81$. Plots show the potential v at time T = 500 msec on the epicardium (left) and the endocardium together with transmural sections (right). Colors range from blue (resting potential = − 84 mV) to red (excitation wavefront).

three horizontal sections corresponding to the epicardium (first row), midwall (second row) and endocardium (third row). The three numbers under each panel are the minimum and maximum value plotted and the step size between contour lines. We also simulated a full cardiac cycle with the Bidomain - LR1 model on a smaller slab of $2 \times 2 \times 0.5\ cm^3$, discretized with a mesh $201 \times 201 \times 51$. The simulation took about 6.4 days on 25 processors of the HP Super-Dome machine.

5.5.3. Simulation of reentry phenomena. – In addition to normal heartbeats, our parallel code is able to reproduce reentry phenomena usually asso-

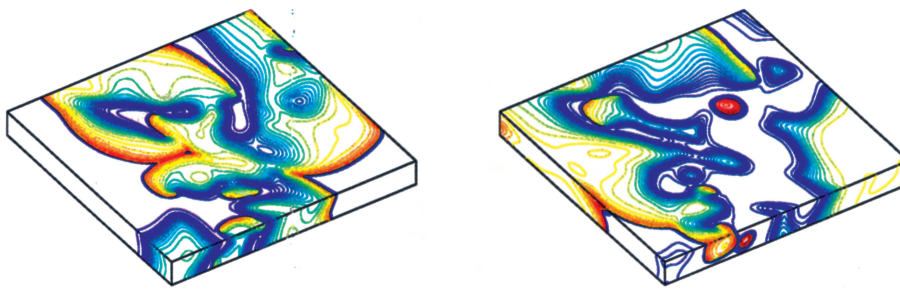

Fig. 6. – Unstable spiral reentry with Monodomain - LR1 model on a domain $6 \times 6 \times 0.6\ cm^3$. Plots show the potential v at times T = 1250 and 1300 msec. Colors range from blue (resting potential = -84 mV) to red (excitation wavefront)

ciated to cardiac arrhythmias such as ventricular tachycardia and fibrillation. Figure 4 shows a stable spiral reentry with the Bidomain - LR1 model on a domain $2 \times 2 \times 0.5\ cm^3$, mesh $201 \cdot 201 \cdot 51$, run on 25 processors of the HP SuperDome machine. The two panels show the transmembrane potential v at times T = 150 and 190 msec; the colors range from blue (resting potential = − 84 mV) to red (excitation wavefront). Figure 5 shows a pair of stable counter-rotating spirals with the Monodomain - LR1 model on an ellipsoidal domain modeling half ventricle (same geometry as in the last case of Table 5) at time $T = 500$ msec after initiation. The mesh employed consists of $501 \times 501 \times 81$ nodes for a total of 20,331,081 unknowns and the model was run on 50 processors of our Linux Cluster, taking about 7.7 sec at each time step. The two plots show the transmembrane potential v on the epicardium (left) and the endocardium together with transmural sections (right), with the same color range as before.

Acknowledgments. The author wishes to thank Piero Colli Franzone, Andrea Toselli, Olof Widlund, and Elena Zampieri for many helpful discussions and suggestions.

REFERENCES

[1] Special issue on *Mapping and control of complex cardiac arrhythmias. Chaos* 12 (3), 2002.
[2] Special issue on *From excitable media to virtual cardiac tissue. Chaos Solit. Frac.* 13 (8), 2002.
[3] Special issue on *Biomedical and bioengineering computing. Comput. Visual. Sci.* 4 (4), 2003.
[4] V. Akcelik et al., *High resolution forward and inverse earthquake modeling on terascale computers.* In Proceedings of SC2003 (Supercomputing Conference 2003), ACM/IEEE, 2003.
[5] O. M. Ascher - S. J. Ruuth - B. T. R. Wetton, *Implicit-explicit methods for time-dependent partial differential equations*, SIAM J. Numer. Anal., **32** (3) (1995), 797-823.
[6] I. Babuška, *Über Schwarzsche Algorithmen in partiellen Differentialgleichungen der mathematischen Physik*, ZAMM, **37** (7/8) (1957), 243-245.
[7] S. Balay - K. Buschelman - W. D. Gropp - D. Kaushik - L. Curfman McInnes - B. F. Smith, *PETSc home page*, http://www.mcs.anl.gov/petsc, 2001.
[8] S. Balay - W. D. Gropp - L. Curfman McInnes - B. F. Smith, *PETSc users manual*, Technical Report ANL-**95/11** - Revision 2.1.0, Argonne National Laboratory, 2001.
[9] C. Bernardi - Y. Maday, *Spectral Methods*, in Handbook of Numerical Analysis, Volume V: Techniques of Scientific Computing (Part 2), North-Holland, 1997, 209-485.

[10] M. BHARDWAJ - D. DAY - C. FARHAT - M. LEISONNE - K. PIERSON - D. RIXEN, *Application of the FETI method to ASCI problems - scalability results on* 1000 *processors and discussion of highly heterogeneous problems*, Int. J. Numer. Meth. Eng., **47** (1-3) (2000), 513-535.

[11] F. BREZZI - M. FORTIN, *Mixed and Hybrid Finite Element Methods*, Springer Series in Computational Mathematics, 15. Springer, New York, 1991.

[12] C. CANUTO - M. Y. HUSSAINI - A. QUARTERONI - T. A. ZANG, *Spectral Methods in Fluid Dynamics*, Springer-Verlag, Berlin, 1988.

[13] T. F. CHAN - T. P. MATHEW, *Domain Decomposition Methods*, Acta Numerica (1994), 61-143.

[14] P. COLLI FRANZONE - L. F. PAVARINO, *A parallel solver for reaction-diffusion systems in computational electrocardiology*, IMATI-CNR Tech. Rep. 9-PV, 2003, To appear in Math. Mod. Meth. Appl. Sci.

[15] P. COLLI FRANZONE - G. SAVARÉ, *Degenerate evolution systems modeling the cardiac electric field at micro and macroscopic level.* In A. Lorenzi and B. Ruf, Editors, Evolution equations, Semigroups and Functional Analysis, 49-78, Birkhauser, 2002.

[16] M. DRYJA - B. F. SMITH - O. B. WIDLUND, *Schwarz analysis of iterative substructuring algorithms for elliptic problems in three dimensions*, SIAM J. Numer. Anal., **31** (1994), 1662-1694.

[17] M. DRYJA - O. B. WIDLUND, *Schwarz methods of Neumann-Neumann type for three-dimensional elliptic finite element problems*, Comm. Pure Appl. Math., **48** (1995), 121-155.

[18] C. FARHAT - F.-X. ROUX, *Implicit parallel processing in structural mechanics*, Comput. Mech. Adv., **2** (1) (1994), 1-124.

[19] A. GARFINKEL - Y.-H. KIM - O. VOROSHILOVSKY - Z. QU - J. R. KIL - M.-H. LEE - H. S. KARAGUEUZIAN - J. N. WEISS . P.-S. CHEN, *Preventing ventricular fibrillation by flattening cardiac restitution*, Proc. Nat. Acad. Sci. USA, **97** (11) (2000), 6061-6066.

[20] P. GOLDFELD - L. F. PAVARINO - O. B. WIDLUND, *Balancing Neumann-Neumann Preconditioners for Mixed Approximations of Heterogeneous Problems in Linear Elasticity*, Numer. Math., **95** (2) (2003), 283-324.

[21] I. HERRERA - D. KEYES - O. WIDLUND - R. YATES, Editors, *Proceedings of the Fourteenth International Conference on Domain Decomposition Methods*, UNAM, Mexico City, 2003.

[22] J. KEENER - J. SNEYD, *Mathematical Physiology*, Springer-Verlag, 1998.

[23] D. E. KEYES, *Terascale implicit methods for partial differential equations.* In X. Feng and T. P. Schulze, Editors, *Recent Advances in Numerical Methods for Partial Differential Equations and Applications*, Contemporary Mathematics, **306**, AMS (2002), 29-84.

[24] R. KORNHUBER - R. H. W. HOPPE - D. E. KEYES - J. PERIAUX - O. PIRONNEAU - J. XU, Editors, *Proceedings of the Fifteenth International Conference on Domain Decomposition Methods*, Lecture Notes in Computational Science and Engineering, Springer, to appear, 2004.

[25] P. LE TALLEC, *Domain decomposition methods in computational mechanics*, Comput. Mech. Adv., **1** (2) (1994), 121-220.

[26] P.-L. LIONS, *On the Schwarz alternating method. I.* In First International Symposium on Domain Decomposition Methods for Partial Differential Equations, R. Glowinski et al., Editors, pp. 1-42, SIAM, Philadelphia, 1988.

[27] C. LUO - Y. RUDY, *A model of the ventricular cardiac action potential: depolarization, repolarization, and their interaction*, Circ. Res., **68** (6) (1991), 1501-1526.

[28] J. MANDEL - M. BREZINA, *Balancing domain decomposition for problems with large jumps in coefficients*, Math. Comp., **65** (1996), 1387-1401.
[29] P. K. MOORE, *An adaptive finite element method for parabolic differential systems: some algorithmic considerations in solving in three space dimensions*, SIAM J. Sci. Comput., **21** (4) (2000), 1567-1586.
[30] L. F. PAVARINO - O. B. WIDLUND, *A polylogarithmic bound for an iterative substructuring method for spectral elements in three dimensions*, SIAM J. Numer. Anal., **33** (4) (1996), 1303-1335.
[31] L. F. PAVARINO, *Neumann-Neumann algorithms for spectral elements in three dimensions*, RAIRO M^2AN, **31** (1997), pp. 471-493.
[32] L. F. PAVARINO - A. TOSELLI, Editors, *Recent Developments in Domain Decomposition Methods*, Lecture Notes in Computational Science and Engineering, vol. 23, Springer-Verlag, 2002.
[33] L. F. PAVARINO - O. B. WIDLUND, *Iterative substructuring methods for spectral element discretizations of elliptic systems. II: Mixed methods for linear elasticity and Stokes flow*, SIAM J. Numer. Anal., **37** (2000), 375-402.
[34] L. F. PAVARINO - O. B. WIDLUND, *Balancing Neumann-Neumann methods for incompressible Stokes equations*, Comm. Pure Appl. Math., **55** (3) (2002), 302-335.
[35] A. QUARTERONI - A. VALLI, *Numerical Approximation of Partial Differential Equations*, Springer-Verlag, Berlin, 1994.
[36] A. QUARTERONI - A. VALLI, *Domain Decomposition Methods for Partial Differential Equations*, Oxford Science Publications, 1999.
[37] H. A. SCHWARZ, *Gesammelte Mathematische Abhandlungen*, volume **2**, pp. 133-143, Springer, 1890.
[38] B. F. SMITH - P. BJØRSTAD - W. D. GROPP, *Domain Decomposition: Parallel Multilevel Methods for Elliptic Partial Differential Equations*, Cambridge University Press, 1996.
[39] S. L. SOBOLEV, *L'algorithme de Schwarz dans la théorie de l'elasticité*, Compt. Rend. Acad. Sci. URSS, **IV** (XIII 6) (1936), 243-246.
[40] A. TOSELLI - O. B. WIDLUND, *Domain Decomposition Methods: Algorithms and Theory*, Springer-Verlag, 2004.
[41] H. M. TUFO - P. F. FISCHER, *Fast parallel direct solvers for coarse grid problems*, J. Paral. Distr. Comput., **61** (2) (2001), 151-177.
[42] A. T. WINFREE, *Electrical turbulence in three-dimensional heart muscle*, Science, **266** (5187) (1994), 1003-1006.
[43] H. YU, *A local space-time adaptive scheme in solving two-dimensional parabolic problems based on domain decomposition methods*, SIAM J. Sci. Comput., **23** (1) (2001), 304-322.

Dipartimento di Matematica, Università di Milano, Via Saldini 50
20133 Milano, Italy. E-mail: pavarino@mat.unimi.it
URL: http://www.mat.unimi.it/∼pavarino

Pervenuta in Redazione
il 10 dicembre 2003